Review

CHARGE CARRIER MOBILITY DYNAMICS IN ORGANIC SEMICONDUCTORS AND SOLAR CELLS

V. Gulbinas

Center for Physical Sciences and Technology, Saulėtekio 3, 10257 Vilnius, Lithuania
Email: vidmantas.gulbinas@ftmc.lt

Charge carrier mobility in organic semiconductors is not a constant value unambigously characterizing some particular material, but depends on the electric field, temperature and even on time after it was generated or injected. The time dependence is particularly important for the thin-film devices where charge carriers pass the organic layer before mobility reaching its stationary value. Here we give a review of experimental techniques with ultrafast time-resolution enabling one to address the mobility kinetics and analyse properties of the time-dependent mobility in conjugated polymers and organic solar cells. We analyse kinetics during the charge carrier generation and extraction of free charge carriers. The mobility typically decreases by several orders of magnitude on a picosecond-nanosecond time scale; however, its kinetics also depends on the investigation technique. The mobility kinetics in blends for bulk heterojunction solar cells strongly depends on the stoichiometric ratio of donor and acceptor materials.

Keywords: charge carrier, mobility, kinetics, ultrafast

PACS: 06.60.Jn, 72.20.Jv, 73.63.–b

1. Introduction

Organic electronics is currently developing in several major directions: organic light emitting diodes (OLED), solar cells, printed electronic devices based on organic thin-film transistors, organic sensors, organic spintronics, etc. [1]. Several companies already use organic light emitting diodes (OLEDs) in display technology. Organic devices in several other areas are on a threshold to mass production, but pilot products are usually still more expensive and less efficient than inorganic ones. However, improvement in the ability to control material parameters could rapidly change the situation. The major advantages of organic devices in comparison with the inorganic analogues are expected to be cheapness and low energy consumption in production, flexibility and easy technology to produce large area devices. All

these advantages are vitally important for solar cells, and this science and technology field is now particularly active.

The operation of the majority of electrical and optoelectrical devices is based on the charge carrier motion, which is determined by the charge carrier mobility characterising the carrier drift in an electric field and the related parameter diffusivity characterising the diffusion rate. Together with the carrier density they determine electrical current, which is among the main parameters of electronic materials. The charge carrier motion mechanism in organic materials is significantly different from that in inorganic semiconductors. Charge carriers in inorganic semiconductors are delocalized, feature wave-like motion, and their mobility is mainly limited by wave scattering by defects, impurities and phonons. Therefore, the mobility typically decreases with temperature

but is independent of the electric field. In organic semiconductors, charge carriers are usually localized on single molecules, on small molecular aggregates or on relatively short polymer segments, and their motion has a stochastic rather than coherent wave-like character. Charge carriers in disordered amorphous materials have slightly different energies when they are situated on different molecules, therefore they occupy low energy sites and carrier motion takes place by thermally- and electric field-activated jumps between those low energy sites. This motion character causes mobility dependence on the electric field and inverse temperature dependence in comparison with classical semiconductors – the mobility increases with temperature.

Carrier mobility in organic semiconductors is typically several orders of magnitude lower than in inorganic ones and this is one of the major obstacles for a wide application of organic semiconductors in electronic devices. Their low carrier mobility limits the current and operation rate of organic field-effect transistors [2]. In the case of organic light-emitting diodes, their high carrier mobility is not so crucially important, but it should be balanced for electrons and holes. But the low carrier mobility is one of the major hindrances for the fabrication of electrically pumped organic lasers [3]; the density of low mobility charge carriers should be very high to ensure a sufficient recombination rate, however, charge carriers then strongly absorb the generated light. In organic solar cells, photogenerated charge carriers should be rapidly extracted before their recombination. Although the geminate and nongeminate recombination processes are still not completely understood (for example, a reduced Langevin recombination coefficient was determined for many blends used as active materials in solar cells [4, 5]), it is clear that the carrier mobility is one of the major parameters governing these processes. Carrier mobility was also suggested to play an important role in carrier photogeneration; according to the Brown–Onsager model, charge carriers should be able to overcome a Coulomb attraction by diffusional motion, before they recombine geminately [6].

Charge carrier diffusivity is another important parameter. It determines such processes as geminate and nongeminate carrier recombination, carrier trapping, carrier separation during dissociation of Coulomb bound charge pair states, formation of electric field screening and depletion areas, etc. For example, we have demonstrated that the carrier diffusion rather than carrier drift is mainly responsible for the dissociation of the interfacial charge-transfer states in blends for solar cells [7]. The common action of the carrier drift and diffusion determines electrical currents and spatial distributions of charges in operating devices. The carrier mobility and diffusion coefficient are interrelated and give a full characterization of the carrier motion.

The charge carrier mobility and their diffusion coefficient, in organic materials, are typically not constant values, but strongly vary during the initial time after their appearance in material. Photogenerated or injected charge carriers experience a sequence of relaxation processes: loss of the state coherence leading to localization, vibrational cooling of ionized molecules, dissociation of charge pair states, relaxation within the energetically and spatially distributed density of states, trapping in energy and spatial traps. These processes occur on femtosecond to microsecond time scales and cause dramatic changes in the carrier mobility and diffusion rate. Therefore charge carriers may pass short distances with high effective mobilities [8, 9]; however, the mobility decreases during this time. Correspondingly, the mobility decreases on a distance scale of several to tens of nanometres when carriers drift in electric fields typical of devices [8]. This makes the mobility dynamics very important for thin-film devices such as OLEDs, solar cells or vertical organic thin-film transistors [10], where charge carriers cross thin organic layers before reaching stationary mobility values [9]. Thus, stationary mobility is often an irrelevant or at least insufficient parameter for the description and modelling the operation of these devices. Effective mobility values may be orders of magnitude higher, but usually are unknown. Namely, this situation may happen at some performance conditions in organic solar cells – charge carriers may be extracted faster than they reach stationary mobility values [11, 12]. Therefore modelling of the solar cell operation requires detailed knowledge of the mobility dynamics. We should also be able to characterize, predict and control the mobility dynamics by developing new better materials required for new better devices.

2. Steady-state charge carrier motion in disordered molecular materials

As discussed, carrier motion may be described by two processes – carrier drift and diffusion. In the simplest case, the carrier mobility and diffusivity are interrelated by the Einstein–Smoluchovski relation [13, 14]

$$\mu/q = D/k_B T, \tag{1}$$

where μ is the carrier mobility, q is the electronic charge, D is the diffusion coefficient, k_B is the Boltzmann constant and T is temperature. The validity of the Einstein relation for organic disordered materials is not straightforward [15, 16], particularly in the case of materials with a complex nanostructured morphology, like bicomponential blends for solar cells.

The current density j may be simply described as

$$j = e\mu n F, \tag{2}$$

where e is the electron charge, n is the carrier density and F is the electric field strength. This expression is typically well valid in the case of classical semiconductors, where mobility is a 'good' parameter, constant in a wide range of electric fields. In the case of organic materials, the situation is more complex. The mobility is not only lower by several orders of magnitude than in classical semiconductors, but also strongly depends on the electric field, and even changes in time after the charge carrier has been inserted or generated. Thus, mobility is a 'bad' parameter, it may be considered as constant only at some conditions, therefore, generally, the carrier density cannot be described by Eq. 2. Nevertheless, mobility is still widely used to describe properties of organic semiconductors, just because we do not have any better parameter.

The difference between mobility in classical and organic materials is determined by a different character of carrier motion. A periodical potential created by atoms of crystalline classical semiconductors causes the formation of extended electronic states, and charge carrier may be considered as delocalized, moving in a wave-like manner. Defects in the crystalline structure or impurities may create trap states, which disturb the wave-like carrier motion (Fig. 1, top).
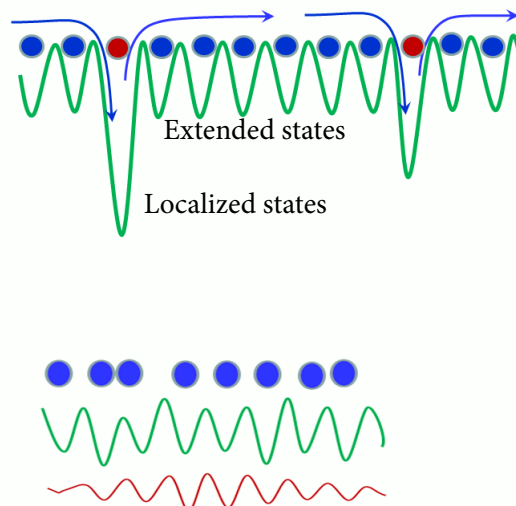

Fig. 1. The top picture demonstrates the trap-controlled carrier motion, and the bottom picture shows the localization of the extended states in disordered materials. Green (online) curves represent the potential surface, the red (online) one shows wave function of the partly localized charge carrier.

If the trap density is high, the carrier motion is trap-controlled. Carriers move with high mobility from one trap to another, and the motion velocity is determined by the trap density and carrier lifetime in a trap. In the case of disordered material, when the potential is not perfectly periodic, the disorder causes localization of wavefunctions (Fig. 1, bottom). Carrier delocalization is now determined by the coupling strength between individual states and by energy disorder. If the disorder is weak in comparison with the coupling, the wavefunctions remain delocalized in some limited space. However, if the disorder is stronger than the coupling, the wavefunctions tend to localize and in extreme cases localize in one site.

Organic semiconductors have a hierarchical structure: coupling between atoms inside an individual molecule is strong, but coupling between molecules is relatively weak, even in the case of molecular solids where molecules are densely packed. In the case of molecular crystals with a highly ordered crystalline structure, the energetic disorder may also be weak therefore carrier delocalization is still possible. However, in amorphous molecular solids, the disorder usually causes a strong carrier localization, usually on a single molecule. Anderson formulated the localization condition stating that a critical intermolecular

coupling V_{jk} exists when charge carriers are localized, related to the width of the distribution of site energies W [17]:

$$\langle V_{jk} \rangle < \alpha^{-1} W. \tag{3}$$

Here α is the coefficient with a value between 6 and 28. Condition (3) may be reformulated in terms of the density of states. The density of states (DOS) of the material describes density in a real space of available energetic states with some particular energy. In the most common case, the material disorder leads to the Gaussian distribution of DOS. It describes the probability to find a state with some particular energy described by the Gaussian function of the energy difference between the state energy and average value of all available states. There is a critical Anderson density of states causing the formation of extended states and thus leading to carrier delocalization. However, this critical DOS value is typically not reached in the case of disordered molecular semiconductors.

The first description of the carrier motion in materials with a high density of deep trap states was developed by Frenkel and Poole [18, 19]. They considered that carrier motion takes place by thermally activated jumps between localized states over the barrier reduced by the applied electric field. The Poole–Frenkel model gives the carrier mobility as a function of temperature and electric field described as

$$\mu = \mu_0 \exp\left(\frac{-q\left(\varphi_{\mathrm{B}} - \sqrt{qE / \pi\epsilon} \right)}{k_{\mathrm{B}}T} \right), \tag{4}$$

where E is the applied electric field, q is the elementary charge, φ_{B} is the voltage barrier, ϵ is the permittivity, and T is the temperature. Bässler has made a step forward to describe the carrier mobility in materials with a Gaussian distribution of DOS [20]. If the DOS distribution is wide, much wider than the thermal energy, charge carriers in equilibrium occupy only the low energy part of the DOS determined by the distribution of DOS and probability of the state occupation described by the Boltzman distribution. Based on the Monte Carlo simulation results, Bässler suggested that carrier mobility might be described as

$$\mu = \mu_\infty \exp\left[-\left(\frac{2\sigma}{3k_{\mathrm{B}}T} \right)^2 + C\left(\left(\frac{\sigma}{k_{\mathrm{B}}T} \right)^2 - \Sigma \right) F^{1/2} \right], \tag{5}$$

where σ is the energetic width of the Gaussian DOS, Σ is the spatial disorder, and C is the scaling factor. This model correctly describes the mobility dependences on the electric field $\ln\mu \sim F^{1/2}$ and the temperature $\ln\mu \sim T^2$, which were confirmed experimentally [21, 22].

3. Time-resolved charge carrier mobility investigation techniques

Conventional electrical charge carrier mobility investigation techniques either measure stationary mobility values or have an insufficient time resolution to address mobility dynamics in organic materials. The time resolution of the electrical methods, when applied to thin molecular films, is typically limited to several nanoseconds. On the other hand, conventional ultrafast spectroscopy techniques, like absorption pump-probe or transient fluorescence, have very limited possibilities to track the carrier motion. Spectroscopic properties of charge carriers (ionized molecules in the case of organic materials) are typically not sensitive to the carrier separation distances once they exceed just the nearest neighbour intermolecular separation. In the best case, one can distinguish between intermolecular charge transfer states and free charge carriers. The transient grating technique, used for the time-resolved investigations of the carrier diffusion rate in classical semiconductors, is also not applicable for organic materials because of too low carrier mobility [23].

Three major ultrafast time-resolved carrier mobility investigation methods have been developed during the last decades: transient photocurrent investigations in the Auston switch configuration [24], mobility probing with ultrashort THz pulses [25, 26] and ultrafast optical electric field probing (UOEFP) by means of the Stark shift [27, 28] or electric field-induced second harmonic (EFISH) generation [8].

3.1. Auston microstrip transmission line technique

The Auston microstrip transmission line technique enabled first carrier motion investigations in organic semiconductors with a better than nanosecond time resolution. Moses et al. [24] used transient photocurrent technique, however, incorporated their samples into the Auston switch. Gold microstrips were deposited directly on the polymer sample leaving a gap from several to tens of micrometres and the sample was fabricated to constitute an electrical transmission line with 50 Ω impedance. Such careful electrical design in some cases enabled better than 100 ps time resolution of photocurrent measurements [29, 30], but demanded a high precision sample preparation. The evaluation of the carrier density was problematic, therefore photocurrent as a product of carrier density and their mobility was typically considered.

3.2. Photoconductivity probing with THz pulses [31]

Photoconductivity probing with THz pulses enabled electrode-free measurements of the sample conductivity kinetics induced by ultrashort optical excitation pulses. This pump-probe-type investigation technique was first introduced to probe carrier dynamics in inorganic semiconductors [32]. A short optical excitation pulse directed to the investigated sample creates bound electron and hole pairs – excitons, and free charge carriers. The induced photoconductivity is probed by the THz radiation pulse propagating through the sample after some variable delay. Intensity, phase shift as well as the frequency of the transmitted THz radiation as a function of the delay time gives the kinetics of the real and imaginary photoconductivity parts. Analysis of both photoconductivity parts enables the separation of inputs of excitons and free charge carriers into the absorption of the THz radiation [33]. Optical excitation and THz probe pulses are usually obtained by using high-power femtosecond lasers. THz radiation is usually generated through an optical rectification process in ZnTe or other nonlinear crystal. Another nonlinear crystal is used for the detection of THz radiation by means of direct electro-optical sampling of the electric field temporal shape. Having additional information on the charge carrier density kinetics, one can evaluate kinetics of the carrier mobility with femtosecond time resolution.

3.3. Ultrafast optical electric field probing (UOEFP)

Ultrafast optical electric field probing (UOEFP) is a modification of the integral-mode transient photocurrent technique, where electric field dynamics in the investigated materials is probed optically instead of photocurrent measurement by a fast oscilloscope. Figure 2 shows the measurement scheme. The investigated material is situated between two electrodes, forming a plate capacitor, which is charged prior to excitation. The created electric field causes the Stark shift of the absorption bands and also breaks the centrosymmetry of the investigated isotropic material enabling electric field-induced second harmonic (EFISH) generation. In the simplest case, both these values show the second power dependence on the electric field strength. Thus, the Stark shift of the absorption bands or EFISH intensity may be used to recalculate the electric field strength. Optical
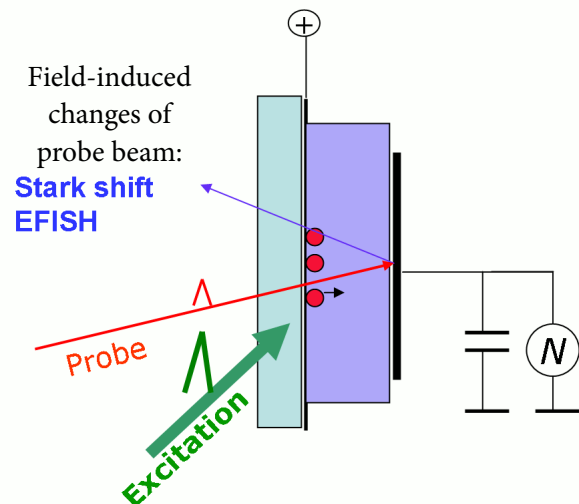

Fig. 2. The UOEFP measurement scheme. The sample film is situated between ITO and metal electrodes. The applied external voltage and different work functions of the electrodes create internal electric field. The excitation pulse photogenerates charge carriers, which by drifting partly discharge the capacitor-like sample. The probe pulse, applied after variable delay, is used to monitor the electric field by measuring the second harmonic generation efficiency or Stark shift of the sample absorption bands.

excitation of the investigated material by an ultrashort laser pulse creates excitons and charge carriers. Both the motion of created charge carriers and the polarization of excitons cause a reduction of the electric field, which may be monitored by the Stark shift [27] or EFISH [29] of the delayed probe pulse. When using femtosecond light pulses for the sample excitation and probing, this technique enables subpicosecond time resolution limited by the duration of excitation and probe pulses. Photocurrent causing the discharge of the plate capacitor-like sample may be calculated as a derivative of the electric field kinetics.

A similar ultrafast time-resolved EFISH probing technique, only without the external electric field, has been also applied by Zhu and co-workers to probe electron transfer at the interface between two molecular layers [34, 35]. An EFISH as a probe was also used to monitor slow electric field dynamics in organic solar cells [36].

The described experimental techniques, although all measure the time dependence of the carrier mobility, give nonequivalent information. In comparison with the Auston microstrip technique, the THz and UOEFP techniques ensure much better time resolution and easier carrier density evaluation. On the other hand, there is a fundamental difference between the UOEFP and THz probing techniques. UOEFP techniques measure carrier motion in the typical device configuration perpendicularly to the thin film, however, they require relatively strong electric fields that may change the real mobility values. THz investigations are performed for electrode-less samples but probe the carrier motion in parallel to the film surface. Both probing methods are expected to give identical results only in the case when charge carriers lose mobility only because of their localization in low energy sites. Thus, in the case of the presence of barriers for the carrier motion, the two methods may give significantly different mobility values and dynamics. This is because THz radiation probes charge carrier motion within short distances of only several nanometres, therefore their motion is insensitive to the barriers if the barrier-free domains are larger. UOEFP probes one-directional carrier motion within distances of tens and hundreds of nanometres and obstacles met in their way rapidly reduce their mobility. This difference is expected to be particularly important

in the case of polymer blends for solar cells, where THz radiation probes carrier mobilities inside single domains, while UOEPF probes carrier motion through the entire blend film, where jumps between domains creating barriers are unavoidable. These differences illustrate that a comprehensive characterization of the carrier motion requires several probing techniques. The time dependence of the mobility obtained by UOEPF is more closely related to the extraction kinetics, at least on a longer time scale. THz photoconductivity measurements mainly reflect the ability of charges to move, whereas UOEPF reflects the transport of charge carriers. The difference between the two measurement techniques reflects the morphology of the blends. The THz technique probes carrier motion inside a single fullerene domain or within a single polymer chain and may remain high if these domains do not contain deep energy traps. In contrast, the mobility revealed by UOEPF decreases with time when carriers performing one-directional motion meet chain ends or domain boundaries, creating obstacles for their motion.

Electric field probing techniques by the EFISH and Stark shift are also not equivalent. The EFISH signal originates from the one-directional macroscopic electric field. On the one hand, it is not sensitive to the electric field variations created by a single charge carrier in its close vicinity. On the other hand, the Stark effect is not sensitive to the electric field direction therefore contributions to the Stark shift give both macroscopic electric field and local fields around charge carriers. Therefore the Stark shift may be observed even in the absence of the macroscopic electric field, as was nicely demonstrated in Ref. [37], where the absolute carrier separation distance during free carrier generation was estimated. It is worth noting that EFISH probing revealing only one-directional carrier motion better characterizes carrier drift dynamics in thin-film devices.

4. Charge carrier photogeneration in organic materials

The charge carrier mobility dynamics is closely related to another important process – charge carrier photogeneration. In the majority of experiments, carrier photogeneration precedes carrier motion, and also the majority of experimental

mobility investigation techniques directly measure the sample photoconductivity, i.e. a product of the carrier mobility and their density, which increases in the course of carrier photogeneration and decreases due to their recombination and extraction. Therefore, prior to discussing the mobility dynamics, a short overview of the carrier generation mechanism in organic materials shall be presented.

Charge carrier photogeneration in organic materials typically does not take place by direct band-to-band transitions like in classical semiconductors, but occurs via an intermediate exciton state. An electron and a hole in the exciton state are bound by the Coulomb attraction force, and the binding energy reaches several hundreds of meV. Therefore, it is not obvious how charge carriers move against mutual electric field attraction overcoming this energy barrier. This issue has been heavily discussed for several decades. A number of carrier generation mechanisms have been suggested. They may be separated into three main groups: a) direct carrier generation by band-to-band transitions, b) charge carrier generation from the nonrelaxed excited state utilizing excess excitation energy for carrier separation, c) charge carrier separation during the entire excited state lifetime driven by thermal energy and external electric field.

4.1. Early models

Charge carrier generation models suggested during the last decades of the 20th century on the base of investigation of photoconductivity of crystalline materials were based on the autoionization mechanism [38] first proposed by Geacintov and Pope [39]. It was assumed that hot charge carriers move away each from other by a significant autoionization distance immediately after generation of a high energy exciton state. This initial separation subsequently allows complete carrier separation according to the Onsager theory [40]. The initial separation was assumed to be mainly driven by the excess vibrational energy, predicting a strong dependence of the dissociation yield on the excitation wavelength. Since such dependence in many materials was not observed, Noolandi and Hong [41] proposed that only a short distance charge transfer (CT) state is created during the electron thermalization, while separation

of the CT state takes place by the Poole–Frenkel process during the long lifetime of the CT state. It was also assumed that the CT state may deactivate only by separating into free charge carriers or by recreating the S_1 state. Popovic suggested an important modification of the model suggesting that the CT state may also decay directly to the ground state [42].

To explain the efficient carrier separation observed in some materials under excitation to the lowest energy absorption band, low energy CT states were suggested as being precursors of charge carriers [43]. Metal phthalocyanines are highly photoconducting materials possessing such low energy CT states. Time-resolved electric-field-induced fluorescence quenching in titanyl phthalocyanine was interpreted as revealing charge carrier photogeneration both from a nonrelaxed CT state and during the entire CT state lifetime [44]. However, investigations of photoconductivity created by two time-correlated short excitation pulses favoured carrier generation only from the nonrelaxed CT state [45].

4.2. Charge carrier generation in conjugated polymers

Charge carrier generation mechanism was particularly intensively investigated in conjugated polymers. A significant carrier delocalization in these materials, extending over several repeat polymer units [46], suggested that the exciton binding energy should be much lower than in other organic materials [47]. Based on a one-dimensional semiconductor model, the direct carrier generation scenario has been suggested, mainly on the basis of the experimental results obtained for polydiaticetylene and poly(paraphenylene vinylene) (PPV) class materials [24, 47, 9]. According to this scenario, charge carrier generation takes place by direct band-to-band transitions instantaneously after photon absorption. On the other hand, a number of more recent investigations supported a molecular picture assuming that charge carrier generation takes place from the exciton state [48]. Two different scenarios of this model were considered. According to one scenario, only hot exciton dissociation is possible, leading to branching into tightly bound luminescent excitons and charge pairs before excitons loose excess vibrational energy [49].

According to another scenario, temperature-assisted dissociation of relaxed singlet excitons may also take place at strong electric field [50, 51]. Direct investigations of the charge carrier generation dynamics by monitoring the appearance and decay of exciton and charge carrier spectral features by means of ultrafast spectroscopy confirmed that the charge carrier generation is more efficient during initial several ps, but the electric field-assisted dissociation of singlet excitons continues during their entire lifetime [52–55]. Moreover, the fast initial dissociation observed under polymer excitation to the lowest excited state was attributed to the system inhomogeneity, rather than to the hot vibrational states [54].

The initial charge carrier separation distance was obtained being only slightly larger than the distance between adjustment polymer chains suggesting that carrier separation takes place by interchain electron transfer [56]. Dissociation of singlet excitons into geminately bounded electron–hole pairs rather than escape of the charge carrier from a columbic well was concluded to be the rate-limiting step of the charge carrier photogeneration [57]. On the other hand, a very fast carrier generation was observed in the m-LPPP polymer under its excitation by UV light to the higher electronic state [58] indicating that branching to the charge pair state and to the lowest exciton state takes place during the high energy exciton relaxation. Figure 3 shows three charge carrier generation routes [58]. Charge carrier generation by the field-assisted barrier crossing takes place under the polymer excitation to the lowest electronic state without significant excess energy. While under excitation to the high energy state, fast and more efficient carrier generation takes place by direct high energy exciton dissociation and by dissociation of the vibrationally hot lowest exciton state.

The above-described investigations addressed intrinsic carrier photogeneration in pure polymers. However, impurities also play a significant role as carrier photogeneration centres. Graupner et al. noticed that oxidation of the m-LPPP polymer, which takes place upon irradiation with visible light in the presence of oxygen, enhances the film photoconductivity by an order of magnitude [50, 60]. However, intrinsic carrier photogeneration and photogeneration by impurities
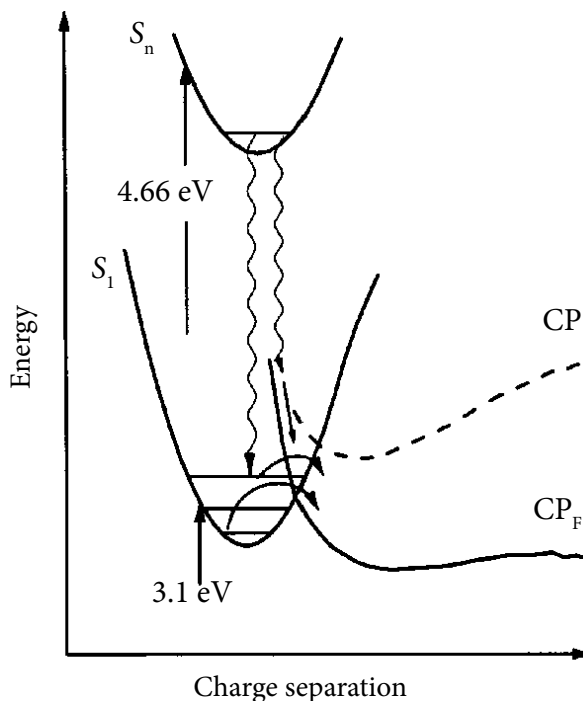

Fig. 3. Charge pair generation model. S_1 and S_n are electronic states localized within a single conjugated polymer segment. CP is a charge pair state and CPF is that modified by the applied electric field [58].

have significantly different properties: generation of charged states at impurities requires no applied electric field or excess energy, and charged species in the m-LPPP were found to appear very rapidly, within 100 fs after photoexcitation [61].

Analysis of the available experimental information allows making a conclusion that the carrier generation in organic semiconductors, including conjugated polymers, shall be considered from a point of view of the molecular approach, considering exciton as a primary photogenerated state involved in the generation of charge carriers. Electric field or temperature assistance are necessary for the exciton dissociation. Therefore, the Onsager model is not directly applicable, since it assumes a field-independent yield of primary photoionization and neglects the field dependence of the initial carrier separation in geminate charge pairs [62, 57].

4.3. Carrier photogeneration in organic solar cells

Carrier photogeneration, as well as their motion processes, are vitally important for organic solar cells (OSC). For efficient OSC the carrier generation efficiency shall be as close to 100% as possible.

In order to increase the generation efficiency, the active layers of OSC are composed of electron-donating and accepting materials, and photoinduced charge separation occurs at their interface. A number of conjugated polymers and glasses of small molecules were used as electron donors, while fullerene derivative PCBM was for a long time strongly dominating as an electron acceptor giving the best cell efficiencies. The first successful attempts to replace fullerene with small organic molecules were reported only in about 2015, and recently all-organic solar cells show record efficiency values reaching 14% [63].

There are two basic architectures of organic solar cells: planar architecture and bulk heterojunction architecture. In planar devices, donor and acceptor layers are deposited on top of each other. Excitons generated in either layer diffuse to the interface where they are separated into an electron and a hole, which drifting in the corresponding layer reach electrodes. This conceptually 'correct' architecture, however, suffers from a small exciton diffusion distance, which is only of about 10–20 nm in disordered organic materials. Therefore, only excitons created close to the interface reach it and contribute to the photocurrent.

In the bulk heterojunction (BHJ) architecture both donor and acceptor materials are mixed together; however, they do not mix to a molecular level but typically form tens of nanometresized interconnected domains. Because of small domain sizes, excitons effectively reach interfaces and split into charge carriers. Electrons and holes drifting via the corresponding material in the electric field created by different electrode work functions reach electrodes creating photocurrent. However, electrons and holes may meet each other by drifting and may recombine. Nevertheless, better efficiencies have been obtained for the BHJ devices, therefore the majority of publications are devoted, to the BHJ devices. A detailed description of all complex processes in organic solar cells is given in numeral reviews [64–66].

Charge carrier generation in OSC is a three-step process: i) a singlet exciton is generated in one of the materials as a result of photon absorption, ii) a singlet exciton, after reaching the donor–acceptor interface, converts into the interfacial CT exciton with an electron in the acceptor material and a hole in the donor material, iii) a CT exciton splits into a pair of a free electron and a hole. The first two steps are very fast and efficient; CT excitons are created dominantly on a femtosecond time scale with close to 100% efficiency in efficient OSC [67, 68]. Taking into account domain sizes being of tens of nm, so fast exciton diffusion is surprising. It suggests that some kind of hybrid states between delocalized Frenkel excitons and CT states may be formed and, thus, coherent exciton transfer may take place. The third step has caused particularly intense debates. This is because the point charge approximation gives the binding energy of several hundreds of meV. It is not easy to understand how charge carriers may overcome tens of times higher than $k_\mathrm{B}T$ barrier and split into an independent free electron and a hole. One of the ideas was that charge carrier separation takes place from some intermediate state [69] prior or in parallel to the formation of the relaxed CT state. To support this mechanism, a fast and efficient charge separation was reported under the excitation of a blend with high photon energy [37, 70–73]. However, the mechanism of the hot state separation has not been clearly explained leaving the subsequent fate of the generated charge pairs unaddressed. Generally, if the separation distance is shorter than the Coulomb attraction radius, charge carriers, upon losing their excess energy, tend to localize back to the countercharge. Monte Carlo simulations have shown that the initial charge carrier separation of the order of several nanometres helps a little for the final electron–hole separation to free charge carriers, unless this distance is comparable with the Coulomb attraction radius [74]. In contrary, other investigations reported charge carrier generation efficiency basically independent of the excess energy suggesting that the relaxed CT excitons are the major precursors of free charge carriers [75–77]. Several factors have been discussed that may reduce the CT state binding energy enabling dissociation of the relaxed CT state: a) a high dielectric permittivity of PCBM [78], b) the delocalization of charge carriers forming CT states [79, 80], c) the formation of interfacial dipoles creating repulsive forces repelling carriers away from the interface [81], d) the increase in entropy during the charge separation, reducing the free energy of separated charges [82, 83].

5. Charge carrier mobility dynamics

5.1. Carrier mobility dynamics in conjugated polymers

The Gaussian disorder model suggested by Bässler predicts that initially photogenerated charge carriers have a higher mobility until they relax to the low energy DOS part. Such relaxation has been demonstrated by Monte Carlo simulations [20]. Moses et al. were the first who experimentally demonstrated the fast photocurrent decay in conjugated polymers excited by ultrashort laser pulses [24]. For explanation, they used the one-dimensional semiconductor model and attributed the strong initial photocurrent to the hot charge carriers in extended band states. Later they demonstrated that charge carriers may drift more than 100 nm with a high mobility before being deep-trapped [9]. A strong, rapidly decaying photocurrent peak initially after photoexcitation was also often observed in conventional time-of-flight measurements [84, 85]. However, usually, not much attention was paid to it since investigations were focused on stationary mobility. Juska et al. have carefully analysed the initial peak, which was observed for two π-conjugated polymers [86] and demonstrated that the initial integrated photocurrent rise observed in the integral mode measurements gives information on the drift distance of nonthermalized carriers. Assuming carrier thermalization time of 100 ps, they evaluated the initial carrier mobility being of about 0.1–0.2 cm²/(Vs).

Although these investigations predicted the carrier mobility decay and gave some estimations of the initial mobility, the mobility dynamics still remained unknown until direct measurements by THz time-domain spectroscopy (THz-TDS) and optical time-resolved electric field probing techniques were applied. The first application of THz-TDS for the investigation of the semiconducting polymer was reported by Hendry et al. [87]. They investigated photoconductivity dynamics in the prototypic photoconducting polymer MEH-PPV film. Analysing real and imaginary photoconductivity dynamics they separated exciton and charge carrier contributions and concluded that charge carriers were generated spontaneously by hot exciton dissociation with the yield of about 1%, but recombined very rapidly on a subpicosecond time scale. The carrier

generation efficiency in an MEH-PPV solution was found being even 3 orders of magnitude lower [88]. The photoinduced conductivity was found being larger and the carrier lifetime much longer, reaching several nanoseconds, in another prototypical polymer RR-P3HT [89]. The larger initial photoconductivity was attributed to the higher initial carrier mobility. These early works, however, were mainly focused on carrier generation rather than on their mobility. A product of the carrier mobility and their density was obtained directly from the experimental data, and the authors used the mobility data from the microwave conductivity investigations at GHz frequencies equal to 0.0025 cm²/(Vs) for MEH-PPV [90] and 0.014 cm²/(Vs) for RR-P3HT [91]. Attempts to evaluate the mobility from the THz-TDS data by application of the Drude–Smith model gave very high values of about 20 cm²/(Vs) for a series of metallated polymers [92] and 30–40 cm²/(Vs) for P3HT [93]. The authors attributed the high mobility to a short-range carrier motion inside highly ordered polymer domains.

The first attempt to address the carrier motion with the ultrafast time resolution by optical probing of the electric field dynamics has been reported in Ref. [27]. The authors have analysed the Stark shift dynamics in the optically excited 100 nm thick m-LPPP polymer sandwiched between ITO and Al electrodes. The stark shift of the polymer absorption band has been observed when samples were charged by 20 V voltage. The Stark shift gradually decreased when charge carriers were photogenerated and by drifting in the electric field discharged the sample capacitance and thus reduced the effective electric field. The quadratic Stark shift was expressed as

$$\Delta G = 1/2\varepsilon_0(\alpha_1 - \alpha_0)E^2, \tag{6}$$

where α_0 and α_1 are the polarizabilities of the conjugated segment in the ground and excited states. The electric field dynamics was recalculated from the experimentally measured Stark shift. On the other hand, the electric field inside the excited polymer film may be expressed as [27]

$$E^* = \frac{2U_{\text{app}}\varepsilon/d - 2n_p er/\varepsilon_0}{1 + \varepsilon - n_p\alpha_0 + n_e(\alpha_1 - \alpha_0)}, \tag{7}$$

where U_{app} is the applied voltage, d is the film thickness, n_e and n_p are the densities of excitons and *e-h*

pairs, respectively, and *r* is the charge carrier separation distance along the electric field direction. The term $n_e(\alpha_1 - \alpha_0)$ here appears because of the exciton contribution, which was evaluated on the basis of the evaluated exciton density and available information on the exciton polarizability [94]. Based on these relations, the time-evolution of the charge separation distance was evaluated, which is presented in Fig. 4.

The exciton and polaron contributions may be also evaluated by accounting for their different
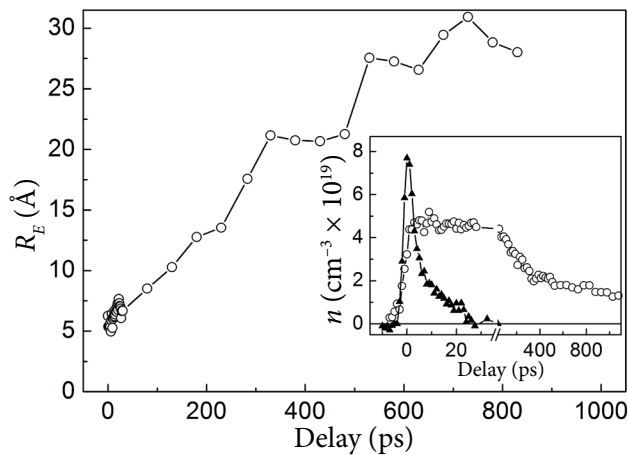
Fig. 4. Dynamics of the average charge separation distance in the m-LPPP film at 25 V of the applied voltage. The inset shows the calculated densities of excitons (triangles) and charge pairs (circles) [27].

temporal and voltage dependences [95]. Figure 5 demonstrates how this procedure was applied to separate the exciton and carrier contribution to the electric field dynamics in the poly-spiro-bifluorene-co-benzothiadiazol (PSF-BT) polymer film, where electric field probing by time-resolved EFISH (TREFISH) was combined with conventional transient photocurrent measurements to evaluate the carrier mobility [13]. Combining the TREFISH and conventional transient photocurrent measurements, carrier mobility dynamics starting from their generation until extraction to electrodes on a microsecond time scale has been evaluated. Figure 6(a) shows that the carrier mobility decreases by about 5 orders of magnitude from 0.1 cm²/(Vs) at 1 ps to 10^{-6} cm²/(Vs) at 1 μs.

Figure 6(b) demonstrates how the carrier mobility decreases as a function of their drift distance. Charge carriers pass 10–20 nm distances with a significantly larger mobility than its stationary
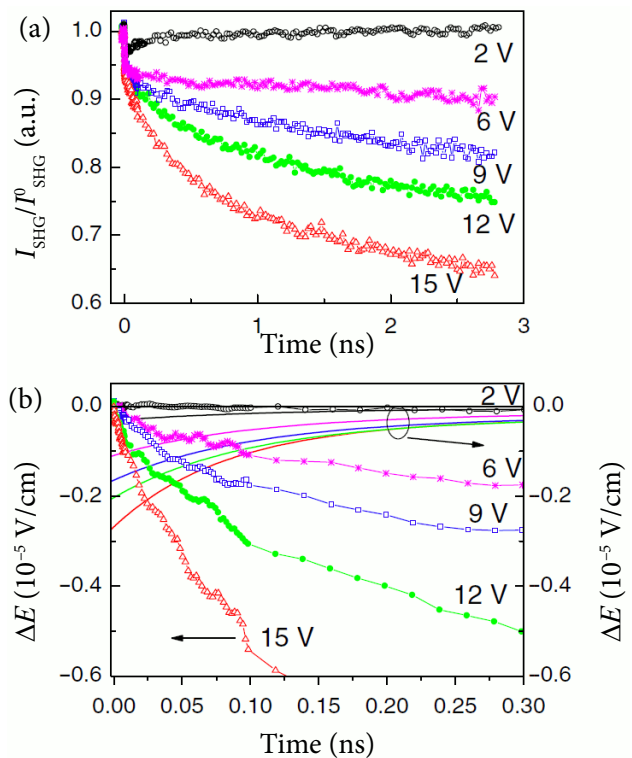
Fig. 5. (a) Kinetics of the second harmonic intensity normalized to that before sample excitation at different applied voltages. (b) Electric field kinetics at early times obtained from the ISHG kinetics. Symbols show the charge-carrier contribution, lines show the exciton contribution [8].

value. This result qualitatively agrees with the fast charge carrier extraction from thin polymer films observed by Moses et al. [9]; however, it demonstrates that the high initial carrier mobility and its dramatic decrease are in agreement with the Gaussian disorder model demonstrating the relaxation of charge carriers within the Gaussian distribution of the density of states. The obtained initial carrier mobility values of about 0.1 cm²/(Vs) are much lower than 600 cm²/(Vs) mobility obtained for the m-LPPP polymer by means of microwave conductivity technique [96], or 5 cm²/(Vs) obtained for single crystals of polydiacetylene(bis p-toluene sulfonate, by means of Auston switch technique [24]. However, they are quite similar as evaluated for MEH-PPV from time-resolved photoconductivity data [9]. Thus, the mobility dynamics obtained for PSF-BT [8] may be considered as representative of disordered conjugated polymers.

Further investigations of the carrier drift dynamics in structurally modified conjugated polymers provided important information about the carrier
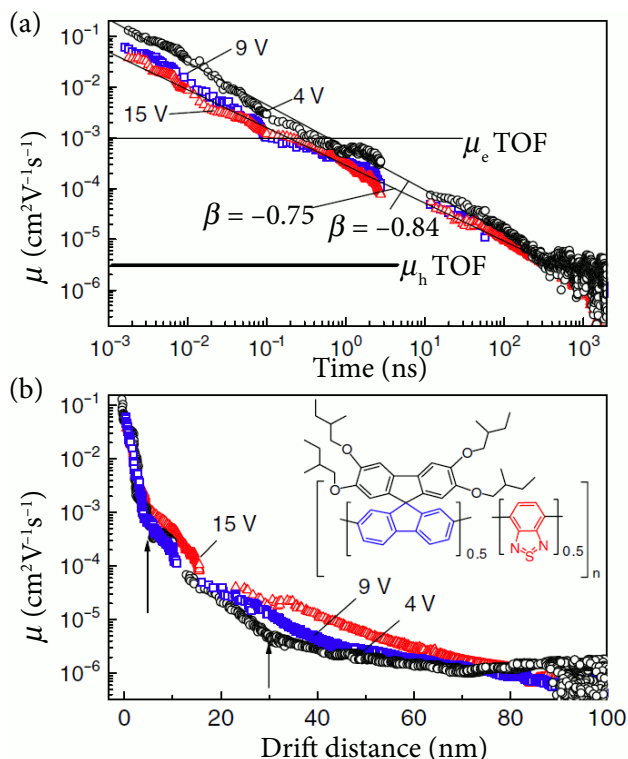
Fig. 6. (a) Carrier mobility kinetics in PSF-BT. Horizontal lines represent the electron and hole mobility as obtained from TOF measurements. (b) Dependence of the mobility on the drift distance. The inset depicts the chemical structure of PSF-BT [8].

motion along conjugated polymer chains and between them. PSF-BT polymer chains were dispersed in electrically isolating polystyrene, and the carrier motion dynamics in such films was compared with the carrier motion dynamics in a pure PSF-BT film [97]. Figure 7 shows the voltage decay kinetics of the electrically charged sample obtained by TREFISH measurements.

The voltage decay kinetics in both samples was surprisingly identical up to several hundreds of picoseconds, indicating that the carriers drifted identically in the isolated photoconducting polymer chains and in the bulk photoconducting polymer. The difference appears only on a timescale of several ns suggesting that interchain carrier jumps become important only in this time domain. To confirm this hypothesis, the F8BT polymer chains were oriented parallel to the substrate plane so that carrier drift in the perpendicularly applied electric field was possible only by the interchain jumps. No fast initial photocurrent component was observed, the substantial carrier drift took place only on a nanosecond time scale. These
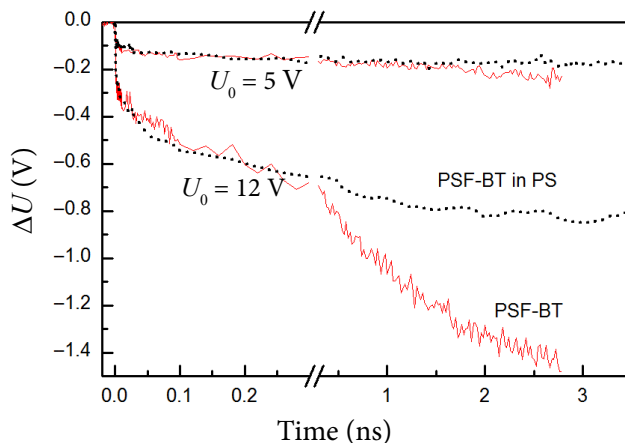

Fig. 7. Voltage attenuation kinetics evaluated from TREFISH measurements in a neat PSF-BT film (solid red (online) lines) and in a non-conducting polystyrene film containing 10% PSF-BT (dot lines) at different applied voltages [97].

findings allowed one to draw the hierarchical carrier motion sketch of the transport processes in the conjugated polymers presented in Fig. 8.

Additional details of the carrier motion mechanism were clarified by investigating temperature dependence of the time-resolved mobility in the same PSF-BT polymer. Previous transient photocurrent investigations of polydiacetylene and PPV polymers have revealed that the initial photocurrent on a ps timescale was independent of temperature [24, 98]. It was attributed to the motion of free charge carriers, before their trapping. Investigations of the PSF-BT polymer by
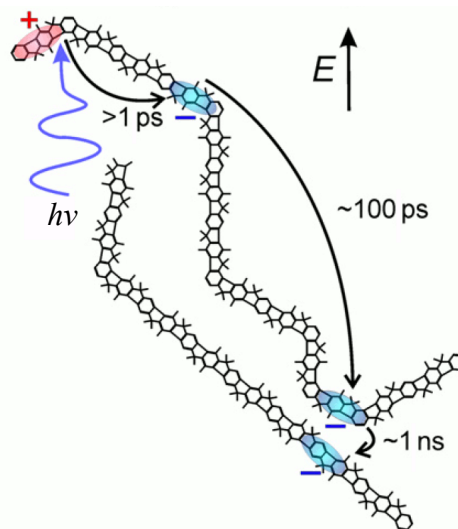

Fig. 8. A sketch of the carrier transport properties in the conjugated polymers [97].

means of TREFISH technique revealed more details of the temperature-independent initial carrier motion [99]. The average carrier drift distance during initial 100–200 ps was found being completely identical within the 10–296 K range (see Fig. 9). The charge carriers drifted approximately 3 nm during this time. Since electrons and holes drift to different directions, the average separation distance along the electric field direction was estimated being of about 6 nm. At longer times, the carrier drift rate was found to increase with temperature in agreement with the Gaussian disorder model.
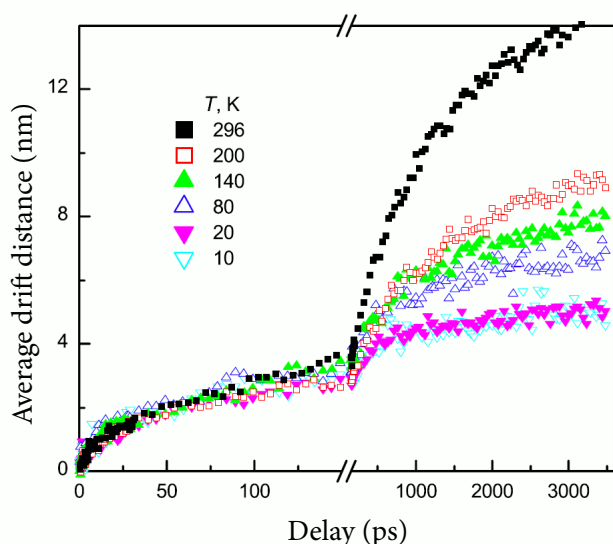

Fig. 9. The average charge carrier drift distance versus time delay after photoexcitation at different temperatures [99].

Since the carrier drift during initial 100 ps was attributed to the intrachain motion, one can conclude that the intrachain carrier motion is independent of temperature, while temperature dependence at longer times originates from the interchain jumps suggesting that barriers for such jumps are equal to about 22 meV. On the other hand, the Gaussian disorder model also predicts the initial carrier mobility being temperature-independent when carriers relax within DOS and dominantly perform down-energy jumps. Nevertheless, the relaxation within DOS is a gradual process lasting until mobility reaches the stationary value, therefore it alone can hardly cause so clear turnover from the temperature-independent to the activated carrier drift. Noriega et al. performed

an analytical and computational description of the carrier dynamics in conjugated polymers and were able to reproduce the experimentally reported carrier mobility dynamics on a wide timescale and its temperature dependence [100]. Their calculations confirmed the above-described hierarchal carrier motion model.

5.2. Carrier mobility dynamics in PCBM

Carrier drift dynamics was also investigated in fullerene derivative 6, 6-phenyl C61-butyric acid methyl ester by probing the electric field dynamics by means of the Stark effect (PCBM). This material for a long time was the main electron acceptor used in organic solar cells. Cabanillas-Gonzalez et al. demonstrated that carrier mobility was constant during initial 5–10 ps, and attributed it to the short-lived high mobility state [28], while mobility decay at longer times was attributed to the carrier trapping. Devizis et al. found that a high and time-independent electron mobility remained until they were extracted from the 40 nm thick PC61BM film during several ps, while a lower mobility at long times was attributed to the motion of holes [101].

5.3. Carrier mobility dynamics in organic solar cells

Although it is clear that carrier mobility plays a very important role in the operation of organic solar cells, this parameter in the case of OSC is even more ambiguous than in the case of neat conjugated polymers. First, it is more ambiguous because of the presence of the intermediate CT state. An electron and a hole are bound together in this state therefore they do not participate in current; however, they may contribute to displacement current because they may have some displacement freedom. Moreover, the experimental separation between free charge carriers and CT states is a difficult task. First, because spectral features of both are very similar. Second, it remains unclear how CT states split into free charge carriers: by long-distance jumps over the barrier or by gradual motion away. It is also not clear how the electric field changes this process if the concept of carrier drift governed by mobility and electric field is applicable in this case. Third, blends are composed of interrelated domains and it remains unclear how

this morphology influences carrier drift on short and long distances. The blend morphology was suggested to cause some unusual mobility properties, for example, the theoretical investigation of Koster predicted that mobility decreases with increasing bias voltage [102]. Forth, solar cells use thin, about 100 nm blend layers, therefore it is difficult to separate electron and hole motions by exciting one side of the layer, as used in TOF investigations of much thicker layers. For these reasons carrier mobility in solar cells is usually investigated by averaging it for all charge carriers, without discriminating between free carriers and those still bound to CT states, as well as between electrons and holes.

The first investigation of the ultrafast time-resolved carrier mobility dynamics in a blend for solar cells has been reported by Ai et al. [103]. They investigated time-resolved THz (TR-THz) photoconductivity dynamics in poly(3-hexylthiophene) (P3HT) blended with PCBM and observed an instantaneous photoconductivity rise and a subsequent decay by 80% during 5 ps. A similar fast photoconductivity decay was reported for some other blends [104, 105]. The fast photoconductivity decay was attributed to the binding of free charge carriers into excitons [106] or to the cooling of initially hot and highly mobile charge carriers [107]. However, careful investigations performed by changing excitation intensity clarified that the fast photoconductivity decay in these measurements was mainly caused by the high excitation intensity required for TR-THz investigations, which caused a nongeminate charge pair recombination taking place on a ps timescale [105]. These investigations performed at low excitation intensity revealed that charge carriers maintained a high mobility of about 0.1 cm²/(Vs) up to several nanoseconds. This result also suggested that carrier mobility decayed due to cooling and trapping on a subnanosecond timescale much slower than reported in previous publications [104, 107]. It should be noted that all the abovementioned investigations were performed in blend films without electrodes and consequently without the electric field. Another important peculiarity of the THz investigations is that they probed carrier motion on a short distance scale of several nanometres. This is particularly important for blend materials where this distance is shorter than electron donor or electron acceptor domain sizes.

More direct information on the carrier motion in operating solar cells was obtained by Amarasinghe Vithanage et al. using the ultrafast time-resolved optical electric field probing TREFISH technique [7]. The charge carrier drift dynamics was investigated in a complete operating P3HT:PCBM solar cell. The carrier drift distance averaged over electrons and holes was directly obtained by optically probing the electric field decay. Figure 10 shows the drift distance dynamics under various strength of the applied electric field.
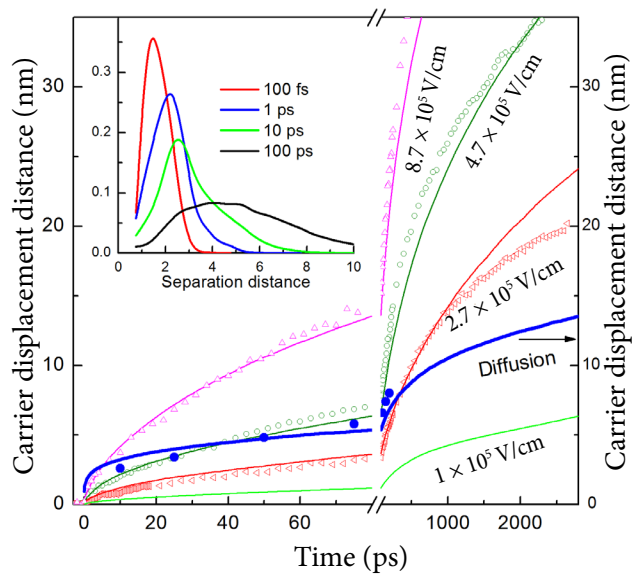

Fig. 10. Time-dependent average charge pair separation distances along the direction of different strength internal electric field (symbols); lines show the dependences obtained by Monte Carlo simulations. A solid blue (online) line shows the simulated absolute carrier separation by diffusion at zero electric field, and blue (online) circles show that calculated from the experimental data by using the Einstein relation. The inset shows the temporal evolution of the distribution of the absolute carrier separation distances at zero electric field [7].

The drift distance increases gradually, without a strong initial jump, which could be expected in the case of ultrafast long-distance carrier separation. At the strong electric field of 8.7×10^5 V/cm, the drift distance reaches about 10 nm during 50 ps; however, at three times weaker field, which is still several times stronger than in operating solar cells, the average drift distance reaches only about 3 nm during 50 ps. It should be noted that the drift distance was averaged over free charge

carriers and charges still remaining bound in CT states, thus the actual drift distance of free charge carriers was larger, especially at initial times. From the drift distance dynamics, the carrier mobility dynamics was evaluated, which is presented in Fig. 11.
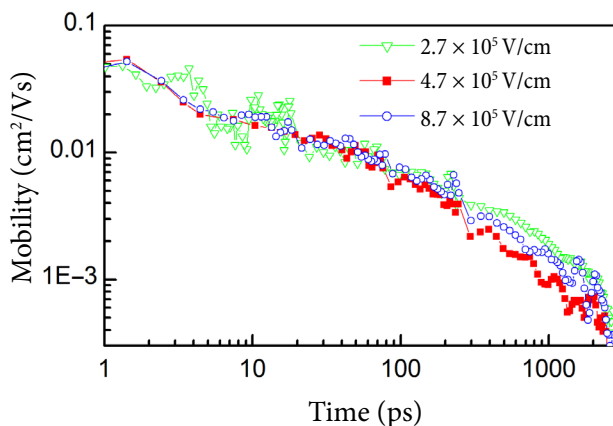

Fig. 11. Time-dependent carrier mobility averaged over electrons and holes determined from the experimental data presented in Fig. 10. Different symbol colours (online) correspond to different field strength [7].

The carrier mobility decreases about 10 times during 100 ps. This is in a stark difference with the investigations by the TR-THz technique, where photoconductivity decay on a picosecond timescale was observed at low excitation intensity [105]. Here it should be noted that TREFISH measurements require much lower excitation intensity than THz measurements, thus the faster mobility decay cannot be an artifact related to recombination. This disagreement clearly shows the difference between the investigation techniques. TR-THz probes carrier mobility inside a single donor or acceptor domain, which decays slowly indicating that carrier trapping is relatively slow. While TREFISH measurements probe one-directional carrier drift, which slows down when carriers reach domain edges, and in order to continue their drift they need to jump to another domain. Combining the information obtained from both techniques, we conclude that the major factor reducing the carrier mobility is barriers between domains rather than carrier trapping and relaxation within DOS. The presence of barriers hampering the carrier motion at longer, microsecond times was recently unambiguously confirmed

by means of modified time-delayed collection field technique [108].

Applying Einstein's relation between the carrier mobility and diffusion coefficient (assuming it is valid for organic materials [109]), the time-dependent diffusion coefficient and the average diffusion distance were calculated. The diffusion distance dynamics for the P3HT:PCBM blend is presented in Fig. 10. At the low electric field of 1×10^5 V/cm, typical of operating solar cells, the diffusion strongly dominates over drift during initial hundreds of ps. Thus, diffusion rather than drift dominates during the splitting time of CT states into free charge carriers.

A different approach to probe charge carrier photogeneration dynamics by means of the optical electric field probing has been suggested by Jailaubekov et al. [34] and by Gélinas et al. [37]. They have investigated ultrafast electric field dynamics at the donor–acceptor interface build-in by separated charge carriers. Jailaubekov et al. used EFISH generation for [34] the investigation of the built-in local electric field at the Cu phthalocyanine/fullerene interface. They demonstrated that hot CT state formation takes place within 100 fs, creating a charge pair with an electron and a hole situated at more distant from the interface molecules; however, during 1 ps this state relaxes to the lowest CT state with the nearest distance electron–hole separation. A similar technique has been also applied by Gélinas et al. [37] to visualize charge separation in a real p-DTS(FBTTh2)2:PC71BM solar cell blend. A careful analysis of the Stark shift contribution into the transient absorption dynamics enabled the estimation of the distance between counter charges during the formation of the interfacial CT state. They estimated that the electron and the hole separate to the distance of about 4 nm during 40 fs and attributed the ultrafast carrier separation to the coherent electron delocalization within PCBM aggregates. A similar ultrafast carrier separation dynamics has been also evaluated by modelling carrier drift in the (P3TI)/(PC71BM) blend measured by the TREFISH technique. The modelling performed by means of the stochastic Schrödinger equation approach confirmed the importance of the coherent carrier propagation leading to the subpicosecond effective charge carrier separation by several nanometres [110].

So far, we have considered the motion of charge carriers without differentiating them into holes and electrons. However, electron and hole mobilities and their time dependences may be significantly different. A separate characterization of the ultrafast electron and hole mobilites in organic solar cells is a complicated task. A separate measurement of the stationary electron and hole mobilities is relatively simple, it can be done by means of the time-of-flight technique creating charge carriers in a thin layer near one of the electrodes. This approach does not work for thin solar cell layers because of their relatively low absorbance, which makes impossible to create carriers only next to one of the electrodes. Other separation approaches should be used.

One such approach was suggested by Pranculis et al. [111]. It was based on the sensitivity of the electron and hole mobilities to the stoichiometric ratio of donor and acceptor materials. A larger content of the electron acceptor material ensuring a good percolation of acceptor domains shall increase the electron mobility, and vice versa, it shall reduce the hole mobility by reducing percolation of donor domains. This approach has been used to separate electron and hole drift kinetics in one of the effective blends for solar cells made from the conjugated polymer APFO3 and PCBM [111]. Figure 12 shows the electric field dynamics in blends with different stoichiometric ratios.

The initial carrier extraction was found being much faster in blends with a higher PCBM content indicating that one type of charge carriers was extracted much faster. The initial mobility increased in blends with a higher content of the electron accepting material, which suggests that the fast carriers were electrons moving via the acceptor material. Their motion becomes fast when a high acceptor material content ensures an almost nonperturbed path, almost like in the pure PCBM, where electron mobility is high [101]. On the other hand, the high content of the electron donor APFO3 does not ensure a fast motion of holes, indicating that hole mobility via the polymer is significantly slower. To better characterize the electron and hole motions, the field dynamics has been modelled approximating electron and hole mobilities by power-law functions $\mu(t) = \mu_0 t^{-\alpha}$, which are typical of carrier mobilities in disordered materials [112]. The modelling re-
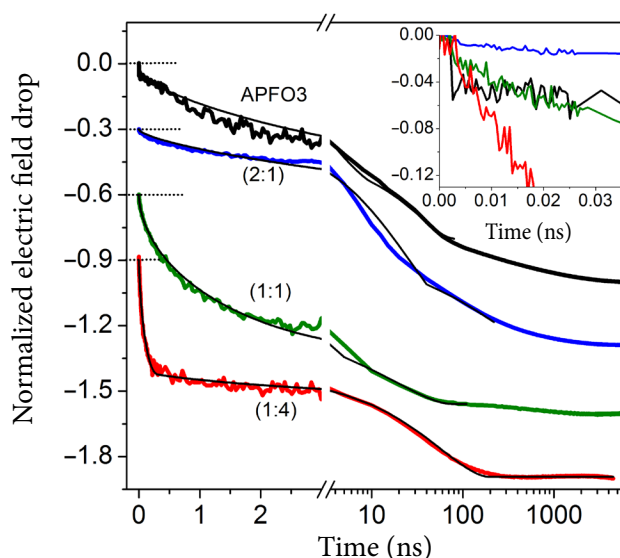

Fig. 12. Normalized electric field kinetics of different blending ratio APFO3:PC61BM cells and of the neat APFO3 film (curves are vertically shifted). The cells were reverse biased at 4 V. Thin black lines show modelled kinetics. The inset shows the initial part of the kinetics, revealing the exciton contribution in the neat polymer film [111].

sults presented in Fig. 13 show that electron mobility is very sensitive to the stoichiometric ratio of the blend increasing by more than 10 times when the PCBM content changes from 33 to 80%. The hole mobility is, however, less sensitive. This difference was attributed to long polymer chains ensuring a better percolation even at a low polymer concentration.

A very similar mobility dependence on the stoichiometric ratio of donor and acceptor materials has been also observed for another polymer PTB7 blend with PC71BM [114] and also for the blends of small molecules merocyanines with fullerenes [115]. These investigations clearly revealed that a high electron mobility of fullerene derivatives being of about 0.1 cm^2/(Vs) at the initial ps time ensures a fast and efficient electron extraction from solar cells. However, the fast electron extraction takes place only in blends with a high concentration (more than 50%) of fullerene or its derivatives. At a low fullerene concentration, both electron mobility and carrier generation drastically decrease, most likely because the CT states formed on a single fullerene molecule recombine rather than split into mobile charge carriers [116].
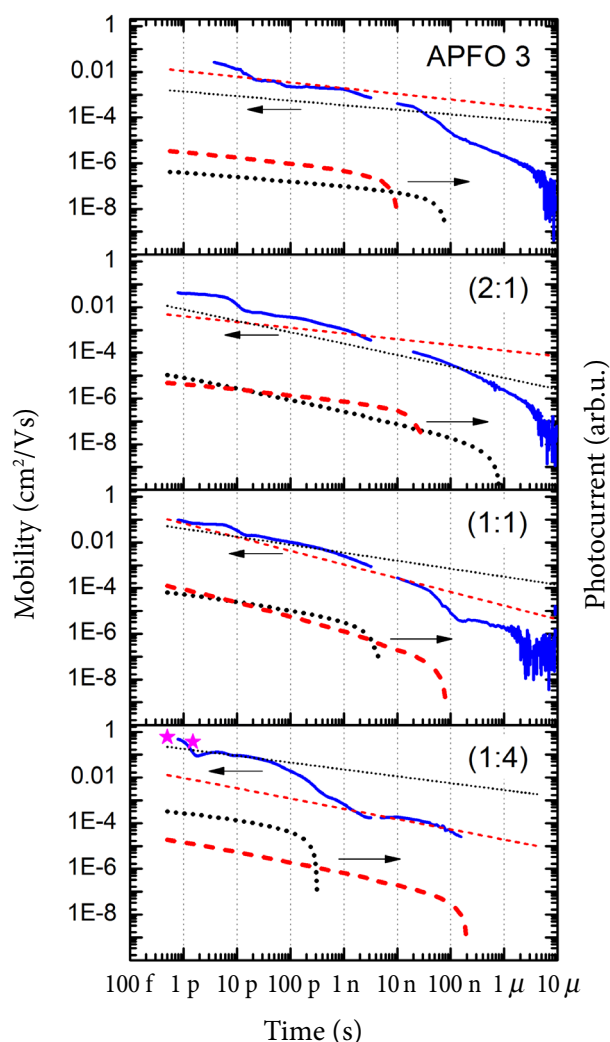
Fig. 13. Experimentally measured average carrier mobility kinetics at 4 V applied voltage ($E \approx 4.8 \times 10^5$ V/cm) in the neat APFO3 and in blends with a different blending ratio (solid blue curves). Red (online) stars show the average carrier mobility of 1:4 device obtained from terahertz spectroscopy measurements [113]. Dashed lines show modelling results. Thin dashed black and red (online) lines are electron and hole mobilities, respectively, while the corresponding thick lines show electron and hole photocurrents [111].

Another approach to separate between electron and hole motion dynamics was applied for a bilayer solar cell in Ref. [117]. Electric field probing by the Stark shift technique was applied to investigate the electric field dynamics in a bilayer organic solar cell composed of a trimethine cyanine dye Cy3 donor layer and a fullerene C60 acceptor layer. Different Stark shift spectra of the trimethine cyanine dye and of fullerene enabled measurements of the electric field dynamics in the cyanine dye and in fullerene layers separately. A clear electric field decay was observed only in the fullerene layer, and this decay was very fast confirming the fast carrier motion in fullerene. In contrast, the carrier motion on a ps timescale in the cyanine dye was negligible. Moreover, a careful analysis of the carrier extraction kinetics from the fullerene layers of different thickness revealed that the extraction rate was limited by the dissociation of the interfacial CT states rather than by electron motion via the fullerene layer. At the low electric field, the CT state dissociation was found to take place during tens and hundreds of picoseconds. This evaluation well agrees with the CT state dissociation time estimated for the bulk heterojunction organic solar cells [7, 118] and confirms that the CT state dissociation is a relatively slow process taking place from the vibrationally relaxed CT state.

6. Summary

The time-resolved mobility investigations revealed that the stationary mobility is not a relevant parameter to describe the charge carrier motion in thin organic films and blends for organic solar cells. The mobility is highly dispersive. The initial mobility of photogenerated charge carriers is initially orders of magnitude higher than expected from the stationary mobility values obtained by steady-state techniques. Charge carriers may pass thin molecular layers before the mobility equilibration. Nevertheless, the role of the fast initial mobility depends on a particular device and its operation conditions. High carrier mobility is not necessary for organic light-emitting diodes, more important is the balance between electron and hole mobilities. However, a low mobility is one of the major obstacles in creation of electrically pumped organic lasers [119]. A fast carrier extraction is very important for the efficient performance of organic solar cells where gradually decreasing carrier mobility causes their dispersive extraction and affects their recombination [120, 121]. On the other hand, Koster et al. [122, 123] argue that nonequilibrium carrier mobility plays a minor role in carrier extraction from operating solar cells, because carrier thermalization is much faster than their extraction. Indeed, the thermalization rate may increase in operating solar cells because solar light constantly generates charge

carriers, which occupy low energy sites in DOS making the carrier equilibration much faster. Thus, the role of the nonequilibrium mobility may depend on the solar cell operation conditions; it may increase at the reduced solar cell illumination.

Currently, it becomes more and more clear that separation of interfacial CT states in organic solar cells takes place from the vibrationally relaxed CT state [124]. But it happens during the carrier relaxation within DOS. Unambiguously, the carrier equilibration plays an important role in their separation, yet we still lack clear understanding of this process.

References

[1] *Organic Electronics*, Nat. Mater., Focus Issue: Vol. **12**, No. 7 (2013).

[2] H. Koezuka, A. Tsumura, and T. Ando, Field-effect transistor with polythiophene thin film, Synth. Met. **18**, 699 (1987), https://doi.org/10.1016/0379-6779(87)90964-7

[3] I.D.W. Samuel and G.A. Turnbull, Organic semiconductor lasers, Chem. Rev. **107**, 1272 (2007), https://doi.org/10.1021/cr050152i

[4] J. Kniepert, M. Schubert, J.C. Blakesley, and D. Neher, Photogeneration and recombination in P3HT/PCBM solar cells probed by time-delayed collection field experiments, J. Phys. Chem. Lett. **2**, 700–705 (2011), https://doi.org/10.1021/jz200155b

[5] D.H.K. Murthy, A. Melianas, Z. Tang, G. Juška, K. Arlauskas, F. Zhang, L.D.A. Siebbeles, O. Inganäs, and T.J. Savenije, Origin of reduced bimolecular recombination in blends of conjugated polymers and fullerenes, Adv. Func. Mat. **23**, 4262 (2013), https://doi.org/10.1002/adfm.201203852

[6] C. Deibel and V. Dyakonov, Polymer–fullerene bulk heterojunction solar cells, Rep. Prog. Phys. **73**, 096401 (2010), https://doi.org/10.1088/0034-4885/73/9/096401

[7] D. Amarasinghe Vithanage, A. Devižis, V. Abramavičius, Y. Infahsaeng, D. Abramavičius, R.C.I. MacKenzie, P.E. Keivanidis, A. Yartsev, D. Hertel, J. Nelson, V. Sundstrom, and V. Gulbinas, Visualizing charge separation in bulk heterojunction organic solar cells, Nat. Commun. **4**, 2334 (2013), https://doi.org/10.1038/ncomms3334

[8] A. Devižis, A. Serbenta, K. Meerholz, D. Hertel, and V. Gulbinas, Ultrafast dynamics of carrier mobility in a conjugated polymer probed at molecular and microscopic length scales, Phys. Rev. Lett. **103**, 027404 (2009), https://doi.org/10.1103/PhysRevLett.103.027404

[9] D. Moses, J. Wang, G. Yu, and A.J. Heeger, Temperature-independent photoconductivity in thin films of semiconducting polymers: photocarrier sweep-out prior to deep trapping, Phys. Rev. Lett. **80**, 2685 (1998), https://doi.org/10.1103/PhysRevLett.80.2685

[10] N. Stutzmann, R.H. Friend, and H. Sirringhaus, Self-aligned, vertical-channel, polymer field-effect transistors, Science **299**, 1881 (2003), https://doi.org/10.1126/science.1081279

[11] A. Melianas, F. Etzold, T.J. Savenije, F. Laquai, O. Inganäs, and M. Kemerink, Photo-generated carriers lose energy during extraction from polymer-fullerene solar cells, Nat. Commun. **6**, 8778 (2015), https://doi.org/10.1038/ncomms9778

[12] A. Melianas, V. Pranculis, A. Devižis, V. Gulbinas, O. Inganäs, and M. Kemerink, Dispersion-dominated photocurrent in polymer: fullerene solar cells, Adv. Func. Mat. **24**, 4507 (2014), https://doi.org/10.1002/adfm.201400404

[13] A. Einstein, Über die von der molekularkinetischen Theorie der Wärme geforderte Bewegung von in ruhenden Flüssigkeiten suspendierten Teilchen, Ann. Phys. **322**, 549–560 (1905), https://doi.org/10.1002/andp.200590005 [in German].

[14] M. von Smoluchowski, Zur kinetischen Theorie der Brownschen Molekularbewegung und der Suspensionen, Ann. Phys. **326**, 756–780 (1906), https://doi.org/10.1002/andp.19063261405 [in German].

[15] Y. Roichman and N. Tessler, Generalized Einstein relation for disordered semiconductors – implications for device performance, Appl. Phys. Lett. **80**, 1948 (2002), https://doi.org/10.1063/1.1461419

[16] G.A.H. Wetzelaer, L.J. Koster, and P.W. Blom, Validity of the Einstein relation in disordered organic semiconductors, Phys. Rev. Lett.

107, 066605 (2011), https://doi.org/10.1103/PhysRevLett.107.066605

[17] P.W. Anderson, Absence of diffusion in certain random lattices, Phys. Rev. **109**, 1492 (1958), https://doi.org/10.1103/PhysRev.109.1492

[18] J. Frenkel, On pre-breakdown phenomena in insulators and electronic semi-conductors, Phys. Rev. **54**, 647–648 (1938), https://doi.org/10.1103/PhysRev.54.647

[19] P. Rottländer, M. Hehn, and A. Schuhl, Determining the interfacial barrier height and its relation to tunnel magnetoresistance, Phys. Rev. B **65**(5), 054422 (2002), https://doi.org/10.1103/PhysRevB.65.054422

[20] H. Bässler, Charge transport in disordered organic photoconductors – A Monte Carlo simulation study, Phys. Status Solidi B **175**, 15 (1993), https://doi.org/10.1002/pssb.2221750102

[21] P.M. Borsenberger, E.H. Magin, and J.J. Fitzgerald, Hole transport in 1,1-bis((di-4-tolylamino)phenyl)cyclohexane (TAPC) doped poly(styrene)s, J. Phys. Chem. **97**, 8250 (1993), https://doi.org/10.1021/j100133a022

[22] W.F. Laquai, G. Wegner, C. Im, H. Bässler, and S. Heun, Comparative study of hole transport in polyspirobifluorene polymers measured by the charge-generation layer time-of-flight technique, J. Appl. Phys. 99, 023712 (2006), https://doi.org/10.1063/1.2165413

[23] A. Miller, in: *Nonlinear Optics in Semiconductors II*, Vol. 59 (Academic Press, 1998) pp. 287–312.

[24] D. Moses, M. Sinclair, and A.J. Heeger, Carrier photogeneration and mobility in polydiacetylene: Fast transient photoconductivity, Phys. Rev. Lett. **58**, 2710 (1987), https://doi.org/10.1103/PhysRevLett.58.2710

[25] O. Esenturk, J.S. Melinger, and E.J. Heilweil, Terahertz mobility measurements on poly-3-hexylthiophene films: Device comparison, molecular weight, and film processing effects, J. Appl. Phys. **103**, 023102 (2008), https://doi.org/10.1063/1.2828028

[26] P. Parkinson, J. Lloyd-Hughes, M.B. Johnston, and L.M. Herz, Efficient generation of charges via below-gap photoexcitation of polymer-fullerene blend films investigated by terahertz spectros-

copy, Phys. Rev. B **78**, 115321 (2008), https://doi.org/10.1103/PhysRevB.78.115321

[27] V. Gulbinas, R. Kananavičius, L. Valkunas, and H. Bässler, Dynamic Stark effect as a probe of the evolution of geminate electron-hole pairs in a conjugated polymer, Phys. Rev. B **66**, 233203 (2002), https://doi.org/10.1103/PhysRevB.66.233203

[28] J. Cabanillas-Gonzalez, T. Virgili, A. Gambetta, G. Lanzani, T.D. Anthopoulos, and D.M. de Leeuw, Photoinduced transient stark spectroscopy in organic semiconductors: A method for charge mobility determination in the picosecond regime, Phys. Rev. Lett. **96**, 106601 (2006), https://doi.org/10.1103/PhysRevLett.96.106601

[29] C.H. Lee, J.Y. Park, Y.W. Park, D. Moses, A.J. Heeger, T. Noguchi, and T. Ohnishi, Polarization dependence of the photoconductivity of stretch-oriented poly(*p*-phenylenevinylene) films, Synth. Met. **101**, 444–445 (1999), https://doi.org/10.1016/S0379-6779(98)01139-4

[30] D. Moses, H. Okumoto, C.H. Lee, A.J. Heeger, T. Ohnishi, and T. Noguchi, Mechanism of carrier generation in poly(phenylene vinylene): Transient photoconductivity and photoluminescence at high electric fields, Phys. Rev. B **54**, 4748–4754 (1996), https://doi.org/10.1103/PhysRevB.54.4748

[31] C.A. Schmuttenmaer, Exploring dynamics in the far-infrared with terahertz spectroscopy, Chem. Rev. **104**, 1759–1779 (2004), https://doi.org/10.1021/cr020685g

[32] M.C. Beard, G.M. Turner, and C.A. Schmuttenmaer, Subpicosecond carrier dynamics in low-temperature grown GaAs as measured by time-resolved terahertz spectroscopy, J. Appl. Phys. **90**, 5915 (2001), https://doi.org/10.1063/1.1416140

[33] E. Hendry, M. Koeberg, J.M. Schins, H.K. Nienhuys, V. Sundström, L.D.A. Siebbeles, and M. Bonn, Interchain effects in the ultrafast photophysics of a semiconducting polymer: THz time-domain spectroscopy of thin films and isolated chains in solution, Phys. Rev. B **71**, 5201 (2005), https://doi.org/10.1103/PhysRevB.71.125201

[34] A.E. Jailaubekov, A.P. Willard, J.R. Tritsch, W.-L. Chan, N. Sai, R. Gearba, L.G. Kaake,

K.J. Williams, K. Leung, P.J. Rossky, and X-Y. Zhu, Hot charge-transfer excitons set the time limit for charge separation at donor/acceptor interfaces in organic photovoltaics, Nature Mater. **12**, 66 (2013), https://doi.org/10.1038/nmat3500

[35] X. Wu, H. Park, X.-Y. Zhu, Probing transient electric fields in photoexcited organic semiconductor thin films and interfaces by time-resolved second harmonic generation, J. Phys. Chem. C **118**, 10670 (2014), https://doi.org/10.1021/jp502381j

[36] D. Taguchi, M. Weis, T. Manaka, and M. Iwamoto, Probing of carrier behavior in organic electroluminescent diode using electric field induced optical second-harmonic generation measurement, Appl. Phys. Lett. **95**, 263310 (2009), https://doi.org/10.1063/1.3277155

[37] S. Gélinas, A. Rao, A. Kumar, S.L. Smith, A.W. Chin, J. Clark, T.S. van der Poll, G.C. Bazan, and R.H. Friend, Ultrafast long-range charge separation in organic semiconductor photovoltaic diodes, Science **343**, 512–516 (2014), https://doi.org/10.1126/science.1246249

[38] E.A. Silinsh and V. Capek, *Organic Molecular Crystals. Interaction, Localization and Transport Phenomena* (AIP Press, New York, 1994).

[39] N.E. Geacintov and M.J. Pope, Generation of charge carriers in anthracene with polarized light, Chem. Phys. **47**, 1194 (1965), https://doi.org/10.1063/1.1712044

[40] L. Onsager, Initial recombination of ions, Phys. Rev. **54**, 554 (1938), https://doi.org/10.1103/PhysRev.54.554

[41] J. Noolandi and K.M. Hong, Theory of photogeneration and fluorescence quenching, J. Chem. Phys. **70**, 3230 (1979), https://doi.org/10.1063/1.437912

[42] Z. Popovic, A study of carrier generation mechanism in *x*-metal-free phthalocyanine, J. Chem. Phys. **78**, 1552 (1983), https://doi.org/10.1063/1.444846

[43] T. Saito, W. Sisk, T. Kobayashi, S. Suzuki, and T. Iwayanagi, Photocarrier generation processes of phthalocyanines studied by photocurrent and electroabsorption measurements, J. Phys. Chem. **97**, 8026 (1993), https://doi.org/10.1021/j100132a036

[44] Z.D. Popovic, M.I. Khan, S.J. Atherton, A.-M. Hor, and J.L. Goodman, Study of carrier generation in titanyl phthalocyanine (TiOPc) by electric-field-induced quenching of integrated and time-resolved fluorescence, J. Phys. Chem. B **102**, 657–663 (1998), https://doi.org/10.1021/jp973188q

[45] V. Gulbinas, R. Jakubenas, S. Pakalnis, and A. Undzenas, Dynamics of charge carrier precursor photogeneration in titanyl phthalocyanine, J. Chem. Phys. **107**, 4927–4933 (1997), https://doi.org/10.1063/1.474856

[46] L. Robins, J. Orenstein, and R. Superfine, Observation of the triplet excited state of a conjugated-polymer crystal, Phys. Rev. Lett. **56**, 1850 (1986), https://doi.org/10.1103/PhysRevLett.56.1850

[47] C.H. Lee, G. Yu, D. Moses, and A.J. Heeger, Picosecond transient photoconductivity in poly(*p*-phenylenevinylene), Phys. Rev. B **49**, 2396–2407 (1994), https://doi.org/10.1103/PhysRevB.49.2396

[48] *Primary Photoexcitations in Conjugated Polymers: Molecular Exciton Versus Semiconductor Band Model*, ed. N.S. Sariciftci (World Scientific, Singapore, 1997).

[49] M. Yan, L.J. Rothberg, F. Papadimitrakopoulos, M.E. Galvin, and T.M. Miller, Spatially indirect excitons as primary photoexcitations in conjugated polymers, Phys. Rev. Lett. **72**, 1104 (1994), https://doi.org/10.1103/PhysRevLett.72.1104

[50] U. Scherf, A. Bohnen, and K. Mullen, Polyarylenes and poly(arylenevinylene)s, 9. The oxidized states of a (1,4-phenylene) ladder polymer, Makromol. Chem. **193**, 1127 (1992), https://doi.org/10.1002/macp.1992.021930511

[51] E.L. Frankevich, A.A. Lymarev, I. Sokolik, F.E. Karasz, S. Blumstengel, R.H. Baughman, and H.H. Hörhold, Polaron-pair generation in poly(phenylene vinylenes), Phys. Rev. B **46**, 9320 (1992), https://doi.org/10.1103/PhysRevB.46.9320

[52] W. Graupner, G. Cerullo, G. Lanzani, M. Nisoli, E.W. List, G. Leising, and S. De Silvestri, Direct observation of ultrafast field-induced charge generation in ladder-type poly(para-phenylene),

Phys. Rev. Lett. **81**, 3259 (1998), https://doi.org/10.1103/PhysRevLett.81.3259

[53] Y. Zaushitsyn, V. Gulbinas, D. Zigmantas, F. Zhang, O. Inganäs, V. Sundström, and A. Yartsev, Ultrafast light-induced charge pair formation dynamics in poly[3-(2'-methoxy-5'-octylphenyl) thiophene], Phys. Rev. B **70**, 075202 (2004), https://doi.org/10.1103/PhysRevB.70.075202

[54] V. Gulbinas, Y. Zaushitsyn, V. Sundström, D. Hertel, H. Bässler, and A. Yartsev, Dynamics of the electric field-assisted charge carrier photogeneration in ladder-type poly(para-phenylene) at a low excitation intensity, Phys. Rev. Lett. **89**, 107401 (2002), https://doi.org/10.1103/PhysRevLett.89.107401

[55] I.G. Scheblykin, A. Yartsev, T. Pullerits, V. Gulbinas, and V. Sundström, Excited state and charge photogeneration dynamics in conjugated polymers, J. Phys. Chem. B **111**, 6303–6321 (2007), https://doi.org/10.1021/jp068864f

[56] V. Gulbinas, R. Kananavičius, L. Valkūnas, H. Bässler, and V. Sundström, Charge carrier photogeneration in conjugated polymer, Mater. Sci. Forum **384–385**, 279–286, (2002), https://doi.org/10.4028/www.scientific.net/MSF.384-385.279

[57] M. Weiter, H.B. Bässler, V. Gulbinas, and U. Scherf, Transient photoconductivity in a film of ladder-type poly-phenylene: Failure of the Onsager approach, Chem. Phys. Lett. **379**, 177–182 (2003), https://doi.org/10.1016/j.cplett.2003.08.043

[58] V. Gulbinas, Y. Zaushitsyn, H. Bässler, A. Yartsev, and V. Sundström, Dynamics of charge pair generation in ladder type poly(para-phenylene) at different excitation photon energies, Phys. Rev. B **70**, 035215 (2004), https://doi.org/10.1103/PhysRevB.70.035215

[59] W. Graupner, S. Eder, M. Mauri, G. Leising, and U. Scherf, Excited states in PPP-type ladderpolymers probed by photoinduced absorption, Synth. Met. **69**, 419 (1995), https://doi.org/10.1016/0379-6779(94)02511-V

[60] W. Graupner, T. Jost, K. Petritsch, S. Tasch, G. Leising, M. Graupner, and A. Hermetter, Optoelectronic properties of polyphenyls, Annu. Tech. Conf. Soc. Plast. Eng. **43**, 1339–1343 (1997).

[61] V. Gulbinas, D. Hertel, A. Yartsev, and V. Sundström, Charge carrier photogeneration and recombination in ladder-type poly(para-phenylene): Interplay between impurities and external electric field, Phys. Rev. B **76**, 235203 (2007), https://doi.org/10.1002/masy.200450802

[62] V. Arkhipov, H. Bässler, E. Emelyanova, D. Hertel, V. Gulbinas, and L. Rothberg, Exciton dissociations in conjugated polymers, Macromol. Symp. **212**, 13–24 (2004).

[63] J. Hou, O. Inganas, R.H. Friend, and F. Gao, Organic solar cells based on non-fullerene acceptors, Nat. Mater. **17**, 119119 (2018), https://doi.org/10.1038/nmat5063

[64] S. Gunes, H. Neugebauer, and N.S. Sariciftci, Conjugated polymer-based organic solar cells, Chem. Rev. **107**, 1324–1338 (2007), https://doi.org/10.1021/cr050149z

[65] H. Bässler and A. Köhler, 'Hot or cold': How do charge transfer states at the donor–acceptor interface of an organic solar dissociate?, Phys. Chem. Chem. Phys. **17**, 28451 (2015), https://doi.org/10.1039/c5cp04110d

[66] C.S. Ponseca Jr., P. Chábera, J. Uhlig, P. Persson, and V. Sundström, Ultrafast electron dynamics in solar energy conversion, Chem. Rev. **117**, 10940–11024 (2017), https://doi.org/10.1021/acs.chemrev.6b00807

[67] C.J. Brabec, G. Zerza, G. Cerullo, S. De Silvestri, S. Luzzati, J.C. Hummelen, and S. Sariciftci, Tracing photoinduced electron transfer process in conjugated polymer/fullerene bulk heterojunctions in real time, Chem. Phys. Lett. **340**, 232 (2001), https://doi.org/10.1016/S0009-2614(01)00431-6

[68] F.L. Zhang, K.G. Jespersen, C. Bjorstrom, M. Svensson, M.R. Andersson, V. Sundstrom, K. Magnusson, E. Moons, A. Yartsev, and O. Inganas, Copolymer/fullerene blends, Adv. Funct. Mater. **16**, 667 (2006), https://doi.org/10.1002/adfm.200500339

[69] R. Hidayat, Y. Nishihara, A. Fujii, M. Ozaki, K. Yoshino, and E. Frankevich, Time-resolved optical and electrical study of second-order processes responsible for the formation of free polarons in conjugated polymers, Phys. Rev.

B **66**, 075214 (2002), https://doi.org/10.1103/PhysRevB.66.075214

[70] S.D. Dimitrov, A.A. Bakulin, C.B. Nielsen, B.C. Schroeder, J.P. Du, H. Bronstein, I. McCulloch, R.H. Friend, and J.R. Durrant, On the energetic dependence of charge separation in low-band-gap polymer/fullerene blends, J. Am. Chem. Soc. **134**, 18189–18192 (2012), https://doi.org/10.1021/ja308177d

[71] G. Grancini, M. Maiuri, D. Fazzi, A. Petrozza, H.-J. Egelhaaf, D. Brida, G. Cerullo, and G. Lanzani, Hot exciton dissociation in polymer solar cells, Nat. Mater. **12**, 29–33 (2013), https://doi.org/10.1038/nmat3502

[72] K. Chen, A.J. Barker, M.E. Reish, K.C. Gordon, and J.M. Hodgkiss, Broadband ultrafast photoluminescence spectroscopy resolves charge photogeneration via delocalized hot excitons in polymer-fullerene photovoltaic blends, J. Am. Chem. Soc. **135**, 18502–18512 (2013), https://doi.org/10.1021/ja408235h

[73] H. Ohkita, S. Cook, Y. Astuti, W. Duffy, S. Tierney, W.M. Zhang, M. Heeney, I. McCulloch, J. Nelson, D.D.C. Bradley, and J.R. Durrant, Charge carrier formation in polythiophene/fullerene blend films studied by transient absorption spectroscopy, J. Am. Chem. Soc. **130**, 3030–3042 (2008), https://doi.org/10.1021/ja076568q

[74] V. Abramavičius, D. Amarasinghe Vithanage, A. Devižis, Y. Infahsaeng, A. Bruno, S. Foster, P.E. Keivanidis, D. Abramavičius, J. Nelson, A. Yartsev, V. Sundstrom, and V. Gulbinas, Carrier motion in as-spun and annealed P3HT:PCBM blends revealed by ultrafast optical electric field probing and Monte Carlo simulations, Phys. Chem. Chem. Phys. **16**, 2686–2692 (2014), https://doi.org/10.1039/C3CP54605E

[75] K. Vandewal, S. Albrecht, E.T. Hoke, K.R. Graham, J. Widmer, J.D. Douglas, M. Schubert, W.R. Mateker, J.T. Bloking, G.F. Burkhard, et al., Efficient charge generation by relaxed charge-transfer states at organic interfaces, Nat. Mater. **13**, 63–68 (2014), https://doi.org/10.1038/nmat3807

[76] A. Armin, M. Velusamy, P. Wolfer, Y.L. Zhang, P.L. Burn, P. Meredith, and A. Pivrikas, Quantum efficiency of organic solar cells: Electro-optical cavity considerations, ACS Photonics **1**, 173–181 (2014), https://doi.org/10.1021/ph400044k

[77] T.G.J. van der Hofstad, D.D. Nuzzo, M. van dez Berg, R.A.J. Janssen, and S.C.J. Meskers, Influence of photon excess energy on charge carrier dynamics in a polymer-fullerene solar cell, Adv. Energy. Mater. **2**, 1095–1099 (2012), https://doi.org/10.1002/aenm.201200030

[78] M.A. Loi, S. Toffanin, M. Muccini, M. Forster, U. Scherf, and M. Scharber, Charge transfer excitons in bulk heterojunctions of a polyfluorene copolymer and a fullerene derivative, Adv. Func. Mater. **17**, 2111–2116 (2007), https://doi.org/10.1002/adfm.200601098

[79] B. Bernardo, D. Cheyns, B. Verreet, R.D. Schaller, B.P. Rand, and N.C. Giebink, Delocalization and dielectric screening of charge transfer states in organic photovoltaic cells, Nat. Commun. **5**, 3245 (2014), https://doi.org/10.1038/ncomms4245

[80] F.-J. Kahle, C. Saller, S. Olthof, C. Li, J. Lebert, S. Weiß, E.M. Herzig, S. Hüttner, K. Meerholz, P. Strohriegl, and A. Köhler, Does electron delocalization influence charge separation at donor-acceptor interfaces in organic photovoltaic cells?, J. Phys. Chem. C **122**, 21792–21802 (2018), https://doi.org/10.1021/acs.jpcc.8b06429

[81] V.I. Arkhipov, P. Heremans, and H. Bässler, Why is exciton dissociation so efficient at the interface between a conjugated polymer and an electron acceptor?, Appl. Phys. Lett. **82**, 4605–4607 (2003), https://doi.org/10.1063/1.1586456

[82] T.M. Clarke and J.R. Durrant, Charge photogeneration in organic solar cells, Chem. Rev. **110**, 6736–6767 (2010), https://doi.org/10.1021/cr900271s

[83] B.A. Gregg, Entropy of charge separation in organic photovoltaic cells: the benefit of higher dimensionality, J. Phys. Chem. Lett. **2**, 3013–3015 (2011), https://doi.org/10.1021/jz2012403

[84] F. Laquai, G. Wegner, C. Im, H. Bässler, and S. Heun, Nondispersive hole transport in carbazole- and anthracene-containing polyspirobifluorene copolymers studied by the charge-generation layer time-of-flight technique, J. Appl. Phys. **99**, 033710 (2006), https://doi.org/10.1063/1.2168590

[85] D. Hertel and H. Bässler, Photoconduction in amorphous organic solids, Chem. Phys. Chem. **9**, 2–26 (2008), https://doi.org/10.1002/cphc.200700575

[86] G. Juska, K. Genevicius, R. Osterbacka, K. Arlauskas, T. Kreouzis, D.D.C. Bradley, and H. Stubb, Initial transport of photogenerated charge carriers in p-conjugated polymers, Phys. Rev. B **67**, 081201 (2003), https://doi.org/10.1103/PhysRevB.67.081201

[87] E. Hendry, J.M. Schins, L.P. Candeias, L.D.A. Siebbeles, and M. Bonn, Efficiency of exciton and charge carrier photogeneration in a semiconducting polymer, Phys. Rev. Lett. **92**, 6601 (2004), https://doi.org/10.1103/PhysRevLett.92.196601

[88] E. Hendry, M. Koeberg, J.M. Schins, H.K. Nienhuys, V. Sundström, L.D.A. Siebbeles, and M. Bonn, Interchain effects in the ultrafast photophysics of a semiconducting polymer: THz time-domain spectroscopy of thin films and isolated chains in solution, Phys. Rev. B **71** 5201 (2005), https://doi.org/10.1103/PhysRevB.71.125201

[89] E. Hendry, M. Koeberg, J.M. Schins, L.D.A. Siebbeles, and M. Bonn, Free carrier photogeneration in polythiophene versus poly(phenylene vinylene) studied with THz spectroscopy, Chem. Phys. Lett. **432**, 441–445 (2006), https://doi.org/10.1016/j.cplett.2006.10.105

[90] J.M. Warman, G.H. Gelinck, and M.P.D. Haas, The mobility and relaxation kinetics of charge carriers in molecular materials studied by means of pulse-radiolysis time-resolved microwave conductivity: Dialkoxy-substituted phenylenevinylene polymers, J. Phys. C **14**, 9935 (2002), https://doi.org/10.1088/0953-8984/14/42/308

[91] G. Dicker, M.P.D. Haas, J.M. Warman, D.M.D. Leeuw, and L.D.A. Siebbeles, The disperse charge-carrier kinetics in regioregular poly(3-hexylthiophene), J. Phys. Chem. B **108**, 17818 (2004), https://doi.org/10.1021/jp046853l

[92] P.D. Cunningham, L.M. Hayden, H.-L. Yip, and A.K.-Y. Jen, Charge carrier dynamics in metalated polymers investigated by optical-pump terahertz-probe spectroscopy, J. Phys. Chem. B **113**, 15427–15432 (2009), https://doi.org/10.1021/jp906454g

[93] P.D. Cunningham and L.M. Hayden, Carrier dynamics resulting from above and below gap excitation of P3HT and P3HT/PCBM investigated by optical-pump terahertz-probe spectroscopy, J. Phys. Chem. C **112**, 7928–7935 (2008), https://doi.org/10.1021/jp711827g

[94] M.G. Harrison, S. Möller, G. Weiser, G. Urbasch, R.F. Mahrt, H. Bässler, and U. Scherf, Electro-optical studies of a soluble conjugated polymer with particularly low intrachain disorder, Phys. Rev. B **60**, 8650 (1999), https://doi.org/10.1103/PhysRevB.60.8650

[95] A. Devižis, A. Serbenta, D. Hertel, and V. Gulbinas, Exciton and polaron contributions to photocurrent in MeLPPP on a picosecond time scale, Mol. Cryst. Liq. Cryst. **496**, 16–24 (2008), https://doi.org/10.1080/15421400802451345

[96] P. Prins, F.C. Grozema, J.M. Schins, S. Patil, U. Scherf, and L.D.A. Siebbeles, High intrachain hole mobility on molecular wires of ladder-type poly(*p*-phenylenes), Phys. Rev. Lett. **96**, 146601 (2006), https://doi.org/10.1103/PhysRevLett.96.146601

[97] A. Devižis, K. Meerholz, D. Hertel, and V. Gulbinas, Hierarchical charge carrier motion in conjugated polymers, Chem. Phys. Lett. **498**, 302–306 (2010), https://doi.org/10.1016/j.cplett.2010.08.071

[98] C.H. Lee, G. Yu, and A.J. Heeger, Persistent photoconductivity in poly(*p*-phenylenevinylene): Spectral response and slow relaxation, Phys. Rev. B **47**, 15543 (1993), https://doi.org/10.1103/PhysRevB.47.15543

[99] A. Devizis, K. Meerholz, D. Hertel, and V. Gulbinas, Ultrafast charge carrier mobility dynamics in poly(spirobifluorene-co-benzothiadiazole): Influence of temperature on initial transport, Phys. Rev. B **82**, 155204 (2010), https://doi.org/10.1103/PhysRevB.82.155204

[100] R. Noriega, A. Salleo, and A.J. Spakowitz, Chain conformations dictate multiscale charge transport phenomena in disordered semiconducting polymers, PNAS **110**, 16315–16320 (2013), https://doi.org/10.1073/pnas.1307158110

[101] A. Devižis, D. Hertel, K. Meerholz, V. Gulbinas, and E. Moser, Time-independent, high

electron mobility in thin PC61BM films: relevance to organic photovoltaics, Org. Electron. **15**, 3729–3734 (2014), https://doi.org/10.1016/j.orgel.2014.10.028

[102] L.J.A. Koster, Charge carrier mobility in disordered organic blends for photovoltaics, Phys. Rev. B **81**, 205318 (2010), https://doi.org/10.1103/PhysRevB.81.205318

[103] X. Ai, M.C. Beard, K.P. Knutsen, S.E. Shaheen, G. Rumbles, and R.J. Ellingson, Photoinduced charge carrier generation in a poly(3-hexylthiophene) and methanofullerene bulk heterojunction investigated by time-resolved terahertz spectroscopy, J. Phys. Chem. B **110**, 25462–25471 (2006), https://doi.org/10.1021/jp065212i

[104] P.D. Cunningham and L.M. Hayden, Carrier dynamics resulting from above and below gap excitation of P3HT and P3HT/PCBM investigated by optical-pump terahertz-probe spectroscopy, J. Phys. Chem. C **112**, 7928–7935 (2008), https://doi.org/10.1021/jp711827g

[105] C.S. Ponseca, A. Yartsev, E. Wang, M.R. Andersson, D. Vithanage, and V. Sundström, Ultrafast terahertz photoconductivity of bulk heterojunction materials reveals high carrier mobility up to nanosecond time scale, J. Am. Chem. Soc. **134**, 11836–11839 (2012), https://doi.org/10.1021/ja301757y

[106] D.G. Cooke, F.C. Krebs, and P.U. Jepsen, Direct observation of sub-100 fs mobile charge generation in a polymer-fullerene film, Phys. Rev. Lett. **108**, 056603 (2012), https://doi.org/10.1103/PhysRevLett.108.056603

[107] H. Němec, H.-K. Nienhuys, F. Zhang, O. Inganäs, A. Yärtsev, and V. Sundström, Charge carrier dynamics in alternating polyfluorene copolymer: fullerene blends probed by terahertz spectroscopy, J. Phys. Chem. C **112**, 6558–6563 (2008), https://doi.org/10.1021/jp710184r

[108] R. Jasiūnas, A. Melianas, Y. Xia, N. Felekidis, V. Gulbinas, and M. Kemerink, Dead ends limit charge carrier extraction from all-polymer bulk heterojunction solar cells, Adv. Electron. Mater. **4**, 1800144 (2018), https://doi.org/10.1002/aelm.201800144

[109] G.A.H. Wetzelaer, L.J.A. Koster, and P.W.M. Blom, Validity of the Einstein relation in disordered organic semiconductors, Phys. Rev. Lett. **107**, 066605 (2011), https://doi.org/10.1103/PhysRevLett.107.066605

[110] V. Abramavicius, V. Pranculis, A. Melianas, O. Inganäs, V. Gulbinas, and D. Abramavicius, Role of coherence and delocalization in photo-induced electron transfer at organic interfaces, Sci. Rep. **6**, 32914 (2016), https://doi.org/10.1038/srep32914

[111] V. Pranculis, Y. Infahsaeng, Z. Tang, A. Devižis, D.A. Vithanage, C.S. Ponseca Jr., O. Inganäs, A.P. Yartsev, V. Gulbinas, and V. Sundström, Charge carrier generation and transport in different stoichiometry APFO3:PC61BM solar cells, J. Am. Chem. Soc. **136**, 11331–11338 (2014), https://doi.org/10.1021/ja503301m

[112] M. Schubert, E. Preis, J. Blakesley, P. Pingel, U. Scherf, and D. Neher, Mobility relaxation and electron trapping in a donor/acceptor copolymer, Phys. Rev. B **87**, 024203 (2013), https://doi.org/10.1103/PhysRevB.87.024203

[113] S. De, T. Pascher, M. Maiti, K.G. Jespersen, T. Kesti, F. Zhang, O. Inganäs, A. Yartsev, and V. Sundström, Geminate charge recombination in alternating polyfluorene copolymer/fullerene blends, J. Am. Chem. Soc. **129**, 8466 (2007), https://doi.org/10.1021/ja068909q

[114] V. Pranculis, A. Ruseckas, D.A. Vithanage, G.J. Hedley, I.D.W. Samuel, and V. Gulbinas, Influence of blend ratio and processing additive on free carrier yield and mobility in PTB7:PC71BM photovoltaic solar cells, J. Phys. Chem. C **120**, 9588–9594 (2016), https://doi.org/10.1021/acs.jpcc.6b01548

[115] R. Augulis, A. Devižis, D. Peckus, V. Gulbinas, D. Hertel, and K. Meerholz, High electron mobility and its role in charge carrier generation in merocyanine/fullerene blend, J. Phys. Chem. C **119**, 5761–5770 (2015), https://doi.org/10.1021/jp5054698

[116] A. Devizis, D. Peckus, D. Hertel, K. Meerholz, and V. Gulbinas, Charge carrier generation and transport in a polyfluorene copolymer with electron donating side groups doped with PCBM,

J. Phys. Chem. **117**, 15871–15878 (2013), https://doi.org/10.1021/jp4014256

[117] A. Devižis, J. De Jonghe-Risse, R. Hany, F. Nuesch, S. Jenatsch, V. Gulbinas, and J.- E. Moser, Dissociation of charge transfer states and carrier separation in bilayer organic solar cells: A time-resolved electroabsorption spectroscopy study, J. Am. Chem. Soc., **137**, 8192–8198 (2015), https://doi.org/10.1021/jacs.5b03682

[118] D.A. Vithanage, A.B. Matheson, V. Pranculis, G.J. Hedley, S.J. Pearson, V. Gulbinas, I.D.W. Samuel, and A. Ruseckas, Barrier-less slow dissociation of photogenerated charge pairs in high-performance polymer-fullerene solar cells, J. Phys. Chem. C **121**, 14060–14065 (2017), https://doi.org/10.1021/acs.jpcc.7b04868

[119] M.A. Baldo, R.J. Holmes, and S.R. Forrest, Prospects for electrically pumped organic lasers, Phys. Rev. B **66**, 035321 (2002), https://doi.org/10.1103/PhysRevB.66.035321

[120] A. Melianas, V. Pranculis, A. Devižis, V. Gulbinas, O. Inganäs, and M. Kemerink, Dispersion-dominated photocurrent in polymer:fullerene solar cells, Adv. Funct. Mater. **24**, 4507–4514 (2014), https://doi.org/10.1002/adfm.201400404

[121] A. Melianas, V. Pranculis, Y. Xia, N. Felekidis, O. Inganäs, V. Gulbinas, and M. Kemerink, Photogenerated carrier mobility significantly exceeds injected carrier mobility in organic solar cells, Adv. Energy Mater. **7**, 160214 (2017), https://doi.org/10.1002/aenm.201602143

[122] N.J. van der Kaap and L.J.A. Koster, Charge carrier thermalization in organic diodes, Sci. Rep. **6**, 19794 (2016), https://doi.org/10.1038/srep19794

[123] V.M. Le Corre, A.R. Chatri, N.Y. Doumon, and L.J.A. Koster, Charge carrier extraction in organic solar cells governed by steady-state mobilities, Adv. Energy Mater. **7,** 1701138 (2017), https://doi.org/10.1002/aenm.201701138

[124] S. Athanasopoulos, F. Schauer, V. Nádaždy, M. Weiß, F.J. Kahle, U. Scherf, H. Bässler, and A. Köhler, What is the Binding Energy of a Charge Transfer State in an Organic Solar Cell, Adv. Energy Mater. **9**, 1900814 (2019), https://doi.org/10.1002/aenm.201900814

Apžvalga

KRŪVININKŲ JUDRIS ORGANINIUOSE PUSLAIDININKIUOSE IR SAULĖS ELEMENTUOSE

V. Gulbinas

Fizinių ir technologijos mokslų centras, Vilnius, Lietuva

Santrauka

Krūvininkų judrio vertė organiniuose puslaidininkiuose nėra pastovi, vienareikšmiškai apibūdinanti medžiagos savybes, tačiau priklauso nuo elektrinio lauko, temperatūros ir netgi po generacijos ar injektavimo bėgant laikui kinta. Judrio laikinė priklausomybė ypač svarbi plonasluoksniams prietaisams, kuriuose krūvininkai pereina organinį sluoksnį greičiau nei nusistovi pusiausviro judrio vertė. Šioje publikacijoje apžvelgiami eksperimentiniai aukštos laikinės skyros krūvininkų judrio tyrimo metodai ir analizuojama judrio kinetika konjuguotuosiuose polimeruose ar organiniuose saulės elementuose krūvininkų generacijos ir ištraukimo metu. Krūvininkų judris kinta keliomis eilėmis pikosekundinėje-nanosekundinėje laiko skalėje, tačiau jo dinamika taip pat priklauso ir nuo tyrimo metodo. Krūvininkų judrio kinetika organiniuose tūrinės heterosandūros saulės elementuose priklauso nuo donorinės ir akceptorinės medžiagų santykio.